

# Tuning-Free Structured Sparse Recovery of Multiple Measurement Vectors using Implicit Regularization

Lakshmi Jayalal<sup>1</sup> Sheetal Kalyani<sup>1</sup>

## Abstract

Recovering jointly sparse signals in the multiple measurement vectors (MMV) setting is a fundamental problem in machine learning, but traditional methods often require careful parameter tuning or prior knowledge of the sparsity of the signal and/or noise variance. We propose a tuning-free framework that leverages implicit regularization (IR) from overparameterization to overcome this limitation. Our approach reparameterizes the estimation matrix into factors that decouple the shared row-support from individual vector entries and applies gradient descent to a standard least-squares objective. We prove that with a sufficiently small and balanced initialization, the optimization dynamics exhibit a “momentum-like” effect where the true support grows significantly faster. Leveraging a Lyapunov-based analysis of the gradient flow, we further establish formal guarantees that the solution trajectory converges towards an idealized row-sparse solution. Empirical results demonstrate that our tuning-free approach achieves performance comparable to optimally tuned established methods. Furthermore, our framework significantly outperforms these baselines in scenarios where accurate priors are unavailable to the baselines.

## 1. Introduction

Recovering structured signals from incomplete linear measurements is a central theme in modern signal processing, compressed sensing, and machine learning. A particularly important setting is the multiple measurement vectors (MMV) problem corresponding to signals sharing a common underlying structure, particularly a shared sparse support. This joint sparsity structure, prevalent in applications from neuroimaging (Chen et al., 2022) to multiple

input multiple-output (MIMO) channel estimation (Yang & Li, 2024) allows for an improved recovery over processing single vectors individually. Classical approaches for MMV including MMV subspace pursuit (M-SP) (Liu et al., 2019), MMV orthogonal matching pursuit (M-OMP) (Zhang et al., 2022; Chen et al., 2020), approximate message passing based MMV (AMP-MMV) (Ziniel & Schniter, 2012) and MMV-FOCal Underdetermined System Solver (M-FOCUSS) introduced by Cotter et al. (2005), often depend on the optimal tuning of regularization parameters or require prior knowledge of the sparsity level. While Bayesian methods like block sparse Bayesian learning extended for MMV (M-BSBL) (Liu et al., 2013) can learn these parameters, they are often susceptible to noise. These limitations motivate the search for robust, tuning-free methods for achieving row sparsity.

An alternative paradigm based on implicit regularization (IR) through overparameterization has emerged with the works of (Arora et al., 2018; 2019; Li et al., 2018). Specifically, gradient descent is used on an overparameterized or factorized representation of the target signal rather than adding explicit penalty terms (like  $\ell_p$  norms) to the loss function to encourage sparsity. The dynamics of the optimization process, often combined with specific initialization strategies or early stopping, implicitly guide the solution towards desirable structures like sparsity or low rank. This phenomenon has been analyzed in context of single measurement vector (SMV) sparse recovery by Vaskevicius et al. (2019); Li et al. (2021); Chou et al. (2023).

Unlike prior implicit regularization analyses in the SMV setting, such as Vaskevicius et al. (2019); Li et al. (2021); Chou et al. (2023), which factorize a single vector under an  $\ell_2$  loss, the MMV problem involves recovering a matrix with a shared row-sparse structure. This shared support couples the optimization dynamics across columns and naturally leads to a Frobenius-norm objective, motivating a parameterization tailored to MMV recovery. Building on these observations, we propose an overparameterized formulation for row-sparse MMV recovery and analyze the resulting implicit regularization induced by gradient descent.

We consider the standard least-squares loss function  $\mathcal{L}(\mathbf{X}) = \|\mathbf{Y} - \mathbf{AX}\|_F^2$  and optimize it using gradient de-

<sup>1</sup>Department of Electrical Engineering, Indian Institute of Technology, Madras, India. Correspondence to: Lakshmi Jayalal <ee19d751@mail.iitm.ac.in>.

scent. We propose a novel overparameterization that leverages the Hadamard product ( $\odot$ ) and Hadamard power ( $\odot^2$ ), which represent element-wise multiplication and product, respectively. This reparameterization is  $\mathbf{X} = (\mathbf{g}^{\odot 2} \mathbf{1}_L) \odot \mathbf{V}$ , where  $\mathbf{1}_L = [1, 1, \dots, 1]_{1 \times L}$  is a row vector of ones that replicates the squared elements of  $\mathbf{g} \in \mathbb{R}^N$  across the columns of  $\mathbf{V} \in \mathbb{R}^{N \times L}$ . The core idea is that the gradient dynamics acting on the vector  $\mathbf{g}$ , which captures the shared row support, will implicitly drive most of its elements towards zero. Due to the multiplicative structure of our parameterization, the corresponding rows of  $\mathbf{V}$  are simultaneously driven to zero, thereby inducing row sparsity in the reconstructed matrix,  $\mathbf{X}$ . This parametrization is designed specifically to handle multiple vectors sharing a common structure, distinguishing it from other IR methods that focus on SMV by factorizing a single vector. Furthermore, it contrasts with matrix and tensor factorization methods that induce a low-rank bias rather than the desired row sparsity.

Our main contributions are: (1) we introduce a novel Hadamard parameterization for the MMV problem and derive its gradient descent update rules; (2) to the best of our knowledge, we are the first to utilize a Lyapunov-based gradient flow analysis in the context of implicit regularization. This approach departs from standard Grönwall-type arguments, yielding initialization values which are practically feasible. We establish formal guarantees that the trajectory approaches an ideal row-sparse solution under a small and balanced initialization; and (3) we further demonstrate the practical effectiveness of our approach through simulations, showing our approach achieves performance comparable to optimally tuned benchmarks (like M-OMP, M-SP, AMP-MMV, M-BSBL and M-FOCUSS) while overcoming their sensitivity to parameter misspecification.

## 2. Related Works

This work builds upon research in several areas, primarily MMV sparse recovery algorithms, IR in machine learning and the techniques used to analyze IR dynamics.

**Sparse MMV Recovery Algorithms:** The challenge of recovering jointly sparse signals from MMV is addressed by diverse algorithms, many adapted from SMV methods. Approaches range from greedy pursuit algorithms like M-SP, and M-OMP to iteratively reweighted least square based M-FOCUSS and Gaussian approximation approaches like AMP-MMV. These traditional approaches often rely on explicit sparsity-promoting penalties (like  $l_p$  norms) or greedy selection rules, sometimes requiring knowledge of the sparsity level or structure. Additionally, frameworks like block sparse Bayesian learning extended for MMV (M-BSBL) (Liu et al., 2013) exploit statistical correlations to learn hyperparameters. But, when relying on estimated priors, frameworks like M-BSBL struggle to maintain accurate re-

covery in low signal to noise ratio (SNR) regimes. Our work offers an alternative by achieving row sparsity implicitly through optimization dynamics.

**Implicit Regularization via Overparameterization:** A significant body of recent work focuses on the phenomenon of implicit regularization (IR), where the dynamics of gradient descent on an overparameterized model find structured solutions without explicit regularizers (Arora et al., 2018; 2019). This effect has been shown to implicitly favor low-rank solutions in matrix sensing (Soltanolkotabi et al., 2023) and tensor sensing (Razin et al., 2021; Hariz et al., 2024). Crucially, implicit regularization has also been investigated for sparse recovery (Li et al., 2021; Zhao et al., 2022; Vaskevicius et al., 2019; Wu et al., 2020) and structured sparse recovery (Li et al., 2023) in the SMV setting. The scale of initialization is a pivotal factor in these processes, often determining the nature of the learned solution. However, the factorizations used in prior work are suboptimal for capturing the joint sparsity structure inherent in MMV applications. Our work addresses this gap by introducing a parameterization specifically designed for this context. In this framework, the dynamics of gradient descent on our proposed factors implicitly promote the row-sparse structure critical for joint recovery.

**Analysis Techniques for Implicit Regularization:** Analyzing the dynamics and convergence of gradient descent in overparameterized models requires specialized techniques. While methods based on Singular Value Decomposition (SVD) (e.g., Arora et al. (2019); Soltanolkotabi et al. (2023); Li et al. (2018)) and direct element-wise analysis (Li et al., 2021; Zhao et al., 2022; Vaskevicius et al., 2019; Li et al., 2023) are effective for some sparse recovery problems, they become intractable for the complex, non-linear parametrization such as the one we propose. We, therefore, adopt a dynamical systems perspective using gradient flow inspired by the works Razin et al. (2021) and Hariz et al. (2024). However, unlike these prior studies which rely on Grönwall's inequality to bound solution trajectories, we employ a Lyapunov-based analysis. This enables us to avoid an exponential dependence on time for initialization and yields practically useful initialization values.

## 3. Preliminaries

We begin by establishing the basic notation followed by the formal definitions necessary for our analysis.

**Notations:** Boldface capital letters are reserved for matrices. Boldface lowercase letters denote vectors, and lowercase letters denote scalars.  $\mathbf{X}^\top$  is the transpose of matrix  $\mathbf{X}$ .  $X_{ij}$  is the  $(i, j)$ -th element of  $\mathbf{X}$ .  $\mathbf{X}_{i:}$  denotes the  $i$ -th row of any matrix  $\mathbf{X}$ .  $\|\cdot\|_F$ ,  $\|\cdot\|_2$  represent the Frobenius norm of a matrix, and the Euclidean norm of a vector.  $\text{diag}(\mathbf{g})$  denotes

a diagonal matrix with vector  $\mathbf{g}$  as its diagonal elements. We use  $\phi(\mathbf{X}) = \|\mathbf{Y} - \mathbf{AX}\|_F^2$  to denote the squared Frobenius norm of the residual  $\mathbf{Y} - \mathbf{AX}$ . The term  $\mathbf{1}_{N \times L}$  is a matrix of all ones of size  $N \times L$ .

With the notation established, we now define  $\mu$ -coherence to characterize the sensing matrix. We also introduce the unbalancedness and row-unbalancedness constants, which are crucial for analyzing the dynamics of our parameterization.

**Definition 3.1** (Mutual coherence). Let  $\mathbf{A} \in \mathbb{R}^{M \times N}$  be a sensing matrix with  $\ell_2$ -normalized columns, i.e.,  $\|\mathbf{A}_{:i}\|_2 = 1$  for all  $i \in [N]$ . The **mutual coherence** of  $\mathbf{A}$  is defined as

$$\mu(\mathbf{A}) = \max_{i \neq j} |\langle \mathbf{A}_{:i}, \mathbf{A}_{:j} \rangle|$$

where  $\mathbf{A}_{:i}$  is the  $i$ -th column of sensing matrix  $\mathbf{A}$  and  $\langle \cdot, \cdot \rangle$  denotes the inner product. This notion of mutual coherence is standard in compressed sensing and has also been adopted in recent analyses of implicit regularization in overparameterized models, e.g., Li et al. (2021). Throughout this work, we assume that the sensing matrix  $\mathbf{A}$  is  $\mu$ -coherent with  $\ell_2$ -normalized columns.

**Definition 3.2.** The constant  $\epsilon(t) \geq 0$  be defined as the unbalancedness constant (introduced by Razin et al. (2021)), where  $\epsilon(t) = \left| \frac{1}{2} \|\mathbf{g}(t)\|_2^2 - \|\mathbf{V}(t)\|_F^2 \right|$  for any time  $t \geq 0$ .

**Definition 3.3.** The constant  $\epsilon_r(t) \geq 0$  be defined as the row-unbalancedness constant, where  $\epsilon_r(t) = \max_{i \in [N]} \left| \frac{1}{2} g_i^2(t) - \sum_j V_{ij}^2(t) \right|$  for any time  $t \geq 0$  and  $\forall i \in [N]$ .

While defined at any time  $t \geq 0$ , we show in Lemma 5.1 that both  $\epsilon(t)$  and  $\epsilon_r(t)$  are conserved quantities under the gradient flow dynamics. Consequently, we treat them as time-invariant constants throughout this work, hence dropping the time index. With these preliminaries established, we now introduce our IR framework for the MMV problem.

## 4. IR-MMV

Consider the task of recovering an MMV  $\mathbf{X} \in \mathbb{R}^{N \times L}$ , characterized by a common sparsity pattern across its rows. The measurement model is given by:

$$\mathbf{Y} = \mathbf{AX} + \mathbf{W}, \quad (1)$$

where  $\mathbf{Y} \in \mathbb{R}^{M \times L}$  is the measurement matrix,  $\mathbf{A} \in \mathbb{R}^{M \times N}$  is the sensing matrix (with  $M \leq N$ ), and  $\mathbf{W} \in \mathbb{R}^{M \times L}$  represents additive measurement noise. The objective is to recover  $\mathbf{X}$ , which is characterized by having at most  $K$  non-zero rows.

Instead of directly optimizing for  $\mathbf{X}$ , we introduce an overparameterized representation of  $\mathbf{X}$  based on a Hadamard product factorization. This reparameterization is designed

---

### Algorithm 1 Implicit Regularization for MMV (IR-MMV)

---

**Input:** Sensing matrix  $\mathbf{A} \in \mathbb{R}^{M \times N}$ , measurement matrix  $\mathbf{Y} \in \mathbb{R}^{M \times L}$

**Initialize:**  $\alpha_V = 5 \times 10^{-4}$ ,  $\alpha_g = \alpha_V \sqrt{2L}$ , learning rates  $\eta_g = \eta_v = 10^{-4}$ , number of iterations  $T = 5 \times 10^6$ ,  $\mathbf{g}(0) \in \mathbb{R}^N$  with  $\mathbf{g}(0) = \alpha_g \mathbf{1}_L$ ,  $\mathbf{V}(0) \in \mathbb{R}^{N \times L}$  with  $\mathbf{V}(0) = \alpha_v \mathbf{1}_{N \times L}$ .

**Reconstruct initial signal:**  $\mathbf{X}(0) = (\mathbf{g}(0)^{\odot 2} \mathbf{1}_L) \odot \mathbf{V}(0)$ .

**for**  $t = 0, 1, \dots, T-1$  **do**

$$\mathbf{\Lambda} \leftarrow \mathbf{A}^\top (\mathbf{Y} - \mathbf{AX})$$

Update parameters:

$$\mathbf{g}(t+1) = \mathbf{g}(t) + 4\eta_g (\mathbf{g}(t) \odot ((\mathbf{\Lambda} \odot \mathbf{V}(t)) \mathbf{1}_L^\top))$$

$$\mathbf{V}(t+1) = \mathbf{V}(t) + 2\eta_v ((\mathbf{g}^{\odot 2}(t+1) \mathbf{1}_L) \odot \mathbf{\Lambda})$$

Reconstruct signal:  $\mathbf{X}(t+1) = (\mathbf{g}^{\odot 2}(t+1) \mathbf{1}_L) \odot \mathbf{V}(t+1)$

**end for**

**Output:** Estimated signal matrix  $\mathbf{X}$ .

---

such that the inherent dynamics of gradient descent implicitly promote row sparsity. Specifically, we propose to factorize  $\mathbf{X}$  as:

$$\mathbf{X} = (\mathbf{g}^{\odot 2} \mathbf{1}_L) \odot \mathbf{V}, \quad (2)$$

where  $\mathbf{g} = [g_1, g_2, \dots, g_N]^\top \in \mathbb{R}^N$  acts as a row-wise scaling vector, and  $\mathbf{V} \in \mathbb{R}^{N \times L}$  is a component matrix. The term  $\mathbf{1}_L = [1, 1, \dots, 1]_{1 \times L}$  ensures that the squared elements of  $\mathbf{g}$  are replicated across columns. The square term on  $\mathbf{g}$  (i.e.,  $\mathbf{g}^{\odot 2}$ ) is introduced to keep the row activations positive. Recall that the proposed reparameterization when applied to gradient descent optimization will implicitly drive elements of  $\mathbf{g}$  corresponding to inactive rows towards zero. This phenomenon will encourage row sparsity in the reconstructed  $\mathbf{X}$ , leveraging the dynamics of the optimization process rather than explicit regularization terms. We define the mean squared loss as:

$$\mathcal{L}(\mathbf{g}, \mathbf{V}) = \|\mathbf{Y} - \mathbf{A}((\mathbf{g}^{\odot 2} \mathbf{1}_L) \odot \mathbf{V})\|_F^2. \quad (3)$$

The optimization is performed using gradient descent on the factors  $\mathbf{g}$  and  $\mathbf{V}$ . At each iteration, the updated factors are used to reconstruct  $\mathbf{X}$ . The gradient descent update rules for  $\mathbf{g}$  and  $\mathbf{V}$  are derived from the loss function  $\mathcal{L}(\mathbf{g}, \mathbf{V})$ . The gradient descent updates for  $\mathbf{g}$  and  $\mathbf{V}$  are:

$$\mathbf{g}(t+1) = \mathbf{g}(t) - \eta_g \nabla_{\mathbf{g}} \mathcal{L}(\mathbf{g}(t), \mathbf{V}(t)) \quad (4)$$

$$\mathbf{V}(t+1) = \mathbf{V}(t) - \eta_v \nabla_{\mathbf{V}} \mathcal{L}(\mathbf{g}(t), \mathbf{V}(t)) \quad (5)$$

The reconstructed signal matrix  $\mathbf{X}$  at time  $t$  is then given by:

$$\mathbf{X}(t+1) = (\mathbf{g}^{\odot 2}(t+1) \mathbf{1}_L) \odot \mathbf{V}(t+1). \quad (6)$$

The approach is outlined in Algorithm 1. In line with the analysis of matrix and tensor factorization by Gunasekar et al. (2017); Arora et al. (2018); Li et al. (2018); Arora et al. (2019); Razin et al. (2021); Hariz et al. (2024), we also model small learning rate for gradient descent through infinitesimal limit, i.e. through gradient flow:

$$\frac{d}{dt}g_l(t) = -\nabla g_l \mathcal{L}(\mathbf{g}(t), \mathbf{V}(t)), \quad (7)$$

$$\frac{d}{dt}V_{lm}(t) = -\nabla V_{lm} \mathcal{L}(\mathbf{g}(t), \mathbf{V}(t)), \quad (8)$$

where  $g_l(t)$  represents the element of factor  $\mathbf{g}$  corresponding to the  $l$ -th element at time  $t$  and  $V_{lm}(t)$  corresponds to the  $(l, m)$ -th element of factor  $\mathbf{V}$  at time  $t$ . In the following section, we will formally analyze the dynamics of gradient flow to show that they guide the solution towards a row-sparse structure.

## 5. Theoretical Analysis

We begin by identifying a key conservation law of the optimization dynamics for the proposed approach. The following lemma shows that the proposed overparameterization preserves a balancedness property, both globally and at the row level, throughout the optimization process.

**Lemma 5.1** (Balancedness). *For the system evolving under continuous gradient flow for the set of update equations (4), (5) and (6), derived from the loss function  $\mathcal{L}(\mathbf{g}, \mathbf{V}) = \|\mathbf{Y} - \mathbf{A}(\mathbf{g}^{\odot 2} \mathbf{1}_L \mathbf{V})\|_F^2$ , the following properties hold for any time  $t \geq 0$*

1. *Global balancedness: The quantity  $\frac{1}{2}\|\mathbf{g}(t)\|_2^2 - \|\mathbf{V}(t)\|_F^2$  is conserved throughout the optimization process:*

$$\frac{1}{2}\|\mathbf{g}(t)\|_2^2 - \|\mathbf{V}(t)\|_F^2 = \frac{1}{2}\|\mathbf{g}(0)\|_2^2 - \|\mathbf{V}(0)\|_F^2$$

2. *Row-wise balancedness: For each individual row  $i \in [N]$ , the quantity  $\frac{1}{2}g_i^2(t) - \sum_{j \in [L]} V_{ij}^2(t)$  is also conserved:*

$$\frac{1}{2}g_i^2(t) - \sum_{j \in [L]} V_{ij}^2(t) = \frac{1}{2}g_i^2(0) - \sum_{j \in [L]} V_{ij}^2(0)$$

*Proof sketch (for detailed proof see B.1).* The result follows by showing that under gradient flow,  $\frac{1}{2} \sum_{l=1}^N \frac{d}{dt} g_l^2(t) = \sum_{l=1}^N \frac{d}{dt} \|\mathbf{V}_{l:}(t)\|_2^2$  for all  $t \geq 0$ .  $\square$

Lemma 5.1 proves that if the parameters are balanced in the beginning at time  $t = 0$  (i.e.,  $\frac{1}{2}\|\mathbf{g}(0)\|_2^2 = \|\mathbf{V}(0)\|_F^2$ ),

then they will remain perfectly balanced over time, meaning  $\frac{1}{2}\|\mathbf{g}(t)\|_2^2 = \|\mathbf{V}(t)\|_F^2$  for all subsequent time steps. It also shows that for each row  $i$ , the relative proportions between the scaling power of  $g_i$  and the “size” of the  $i$ -th row of  $\mathbf{V}$  (captured by its squared Frobenius norm) are preserved during learning. Here, the proposed IR mechanism for inducing sparsity acts consistently at a row-level. If the optimization drives  $g_i(t)$  towards zero for a particular row  $i$ , then, due to the row-wise balancedness, the corresponding row  $\mathbf{V}_{i:}$  must also approach zero, causing the entire  $i$ -th row of  $\mathbf{X}$  to become sparse.

*Remark 5.2.* In the general case,  $\epsilon$  and  $\epsilon_r$  are independent quantities. However, under the specific initialization of Algorithm 1 (where  $\mathbf{g}(0)$  and  $\mathbf{V}(0)$  are initialized with constant values  $\alpha_g$  and  $\alpha_V$ ), it strictly holds that  $\epsilon_r \leq \epsilon$  for all  $t \geq 0$ . (See Appendix B for the proof.)

We now characterize how the norms of individual rows of the reconstructed signal evolve under gradient flow. The next lemma provides upper and lower bounds on the rate of change of each row norm.

**Theorem 5.3** (Dynamics of row norm). *Consider a system evolving under continuous gradient flow with update equations (4), (5) and (6) with initialization  $\mathbf{g}(0) = \alpha_g \mathbf{1}_L$  and  $\mathbf{V}(0) = \alpha_V \mathbf{1}_{N \times L}$  where  $\alpha_g$  and  $\alpha_V$  are small positive scalars. Let  $\mathbf{\Lambda}(t) := \mathbf{A}^\top (\mathbf{Y} - \mathbf{A}(\mathbf{g}(t)^{\odot 2} \mathbf{1}_L \odot \mathbf{V}(t)))$  and  $\mathbf{\lambda}_i(t)$  denote the  $i$ -th row of  $\mathbf{\Lambda}(t)$ , and*

$$\hat{\mathbf{x}}_i(t) := \begin{cases} \frac{\mathbf{X}_{i:}(t)}{\|\mathbf{X}_{i:}(t)\|_2} & \text{if } \|\mathbf{X}_{i:}(t)\|_2 \neq 0 \\ \mathbf{0} & \text{if } \|\mathbf{X}_{i:}(t)\|_2 = 0 \end{cases}. \quad (9)$$

*Then, for any time  $t \geq 0$  and for all  $i \in [N]$  where  $g_i^2(t) > 0$  and  $\sum_{m \in [N]} V_{im}^2(t) > 0$ , if  $\langle \mathbf{\lambda}_i(t), \hat{\mathbf{x}}_i(t) \rangle \geq 0$  then,*

$$\frac{d}{dt} \|\mathbf{X}_{i:}(t)\|_2 \leq 24 \langle \mathbf{\lambda}_i(t), \hat{\mathbf{x}}_i(t) \rangle \left( \epsilon + \|\mathbf{X}_{i:}(t)\|_2^{2/3} \right)^2 \quad (10)$$

$$\frac{d}{dt} \|\mathbf{X}_{i:}(t)\|_2 \geq 6 \langle \mathbf{\lambda}_i(t), \hat{\mathbf{x}}_i(t) \rangle \left( \frac{\|\mathbf{X}_{i:}(t)\|_2^2}{\epsilon + \|\mathbf{X}_{i:}(t)\|_2^{2/3}} \right), \quad (11)$$

*and if  $\langle \mathbf{\lambda}_i(t), \hat{\mathbf{x}}_i(t) \rangle < 0$  then,*

$$\frac{d}{dt} \|\mathbf{X}_{i:}(t)\|_2 \geq 24 \langle \mathbf{\lambda}_i(t), \hat{\mathbf{x}}_i(t) \rangle \left( \epsilon + \|\mathbf{X}_{i:}(t)\|_2^{2/3} \right)^2 \quad (12)$$

$$\frac{d}{dt} \|\mathbf{X}_{i:}(t)\|_2 \leq 6 \langle \mathbf{\lambda}_i(t), \hat{\mathbf{x}}_i(t) \rangle \left( \frac{\|\mathbf{X}_{i:}(t)\|_2^2}{\epsilon + \|\mathbf{X}_{i:}(t)\|_2^{2/3}} \right). \quad (13)$$

*Proof sketch (for detailed proof see Theorem B.4).* The proof begins by expressing the time derivative of the row norm,  $\frac{d}{dt} \|\mathbf{X}_{i:}(t)\|_2$ , in terms of the underlying parameters  $g_i(t)$  and  $\sum_j V_{ij}(t)$ . The upper and lower bounds are then established by relating the parameter norms ( $g_i^2$  and  $\sum_j V_{ij}^2$ ) back to the matrix row norm ( $\|\mathbf{X}_{i:}\|_2$ ) using the row-unbalancedness constant,  $\epsilon$ .  $\square$

To gain further insight into the row-wise dynamics, we next consider the special case of perfect row-balancedness. Under this condition, the evolution of each row norm admits a simplified and more explicit characterization.

**Corollary 5.4** (Dynamics of row norms under perfect balancedness). *Assume that the system evolves under continuous gradient flow, as described in Lemma 5.1, with perfect row balancedness, i.e.,  $\frac{1}{2}g_i^2(t) = \sum_{j \in [L]} V_{ij}^2(t)$  for all  $i \in [N]$*

*and for any time  $t \geq 0$ . Then, the rate of change of the Euclidean norm of the  $i$ -th row of  $\mathbf{X}(t)$  is characterized by:*

$$\frac{d}{dt} \|\mathbf{X}_{i:}(t)\|_2 = 2^{2/3} 6 \langle \mathbf{\lambda}(t), \hat{\mathbf{x}}_i(t) \rangle \|\mathbf{X}_{i:}(t)\|_2^{4/3}. \quad (14)$$

*Proof sketch (for detailed proof see Corollary B.5).* The proof begins by expressing the derivative  $\frac{d}{dt} \|\mathbf{X}_{i:}(t)\|_2$  in terms of the underlying parameters  $(\mathbf{g}(t), \mathbf{V}(t))$ . Then the result follows by applying row-balancedness assumption and substituting back the row norm.  $\square$

Theorem 5.3 and Corollary 5.4 show that the evolution rate of each row's norm is roughly proportional to its current norm raised to the power  $4/3$ . This implies that when the unbalancedness constant is small, this proportionality creates a “momentum-like” effect: smaller row norms evolve more slowly, while larger row norms change more rapidly. This dynamic, in turn, fosters an incremental learning effect: a phenomenon where different parts of the signal are learned sequentially rather than all at once. This process is realized by certain rows growing significantly in magnitude while others remain small, ultimately leading to an implicit regularization that favors low-rank solutions. The following lemma connects the behavior of the optimization in parameter space to the evolution of the reconstructed signal. It shows that the distance between two signal trajectories can be upper-bounded by the distance between their corresponding parameters.

**Lemma 5.5** (Distance bound in terms of parameters). *Let the estimated trajectory,  $\mathbf{X}(t)$  be parametrized by  $(\mathbf{g}(t), \mathbf{V}(t))$  and a reference trajectory  $\tilde{\mathbf{X}}(t)$ , be parameterized by  $(\tilde{\mathbf{g}}(t), \tilde{\mathbf{V}}(t))$  both of which evolve under the continuous gradient flow, as described in Lemma 5.1. Let  $T > 0$  and  $D > 0$  be scalars. Specifically, assume*

*that for all  $t \in [0, T]$  and all  $n \in [N]$ , the condition  $\max \{ |g_n(t)|, \|V_{n:}(t)\|_2, |\tilde{g}_n(t)|, \|\tilde{V}_{n:}(t)\|_2 \} \leq D$  holds. Then at any time  $t \in [0, T]$ , the following inequality holds:*

$$\|\mathbf{X}(t) - \tilde{\mathbf{X}}(t)\|_F^2 \leq 8D^4 \left\| (\mathbf{g}(t), \mathbf{V}(t)) - (\tilde{\mathbf{g}}(t), \tilde{\mathbf{V}}(t)) \right\|^2, \quad (15)$$

$$\text{where, } \left\| (\mathbf{g}(t), \mathbf{V}(t)) - (\tilde{\mathbf{g}}(t), \tilde{\mathbf{V}}(t)) \right\|^2 = \sum_{n \in [N]} \sum_{l \in [L]} \left( (V_{nl}(t) - \tilde{V}_{nl}(t))^2 + (g_n(t) - \tilde{g}_n(t))^2 \right).$$

*Proof sketch (for detailed proof see Lemma C.2).* The proof begins by substituting the parameterizations for  $\mathbf{X}(t)$  and  $\tilde{\mathbf{X}}(t)$  into the squared Frobenius distance,  $\|\mathbf{X}(t) - \tilde{\mathbf{X}}(t)\|_F^2$ . The result then follows from an algebraic rearranging of terms and the application of standard norm inequalities, including the triangle inequality.  $\square$

This provides the necessary link between the matrix trajectories and their underlying parameters, thus serving as the final component required for the convergence analysis. Specifically, the lemma bounds the distance between the reference trajectory,  $\tilde{\mathbf{X}}(t)$ , and the estimated trajectory,  $\mathbf{X}(t)$  by the distance between their respective underlying parameters  $(\mathbf{g}(t), \mathbf{V}(t))$ ,  $(\tilde{\mathbf{g}}(t), \tilde{\mathbf{V}}(t))$ . Building on this analysis, the following theorem establishes our main convergence guarantee.

**Theorem 5.6.** *Consider the system evolving under continuous gradient flow, where parameters are initialized such that perfect row-balancedness holds for all rows, i.e.,  $\frac{1}{2}g_i^2(0) = \sum_{j \in [L]} V_{ij}^2(0)$  for all  $i \in [N]$ . Let the sensing matrix  $\mathbf{A}$  have  $\ell_2$ -normalized columns and be  $\mu$ -coherent. Let  $\mathbf{X}(t) \in \mathbb{R}^{N \times L}$  be the estimated trajectory obtained by the gradient flow with the proposed parameterization  $\mathbf{X}(t) = (\mathbf{g}(t) \odot^2 \mathbf{1}_L) \odot \mathbf{V}(t)$ . If the initial value  $\alpha_V, \alpha_g$  (where  $g(0) = \alpha_g \mathbf{1}_L$  and  $V(0) = \alpha_V \mathbf{1}_{N \times L}$ , and  $\alpha_V = \frac{1}{\sqrt{2L}} \alpha_g$ ) is sufficiently small, specifically satisfying:*

$$\alpha_V \leq \frac{\epsilon_{app}}{4D^2 \sqrt{2NL(2L+1)}}, \quad (16)$$

*where  $\epsilon_{app} \in (0, 1)$ , then for time  $T > 0$ , there exists a rank- $K$  trajectory  $\tilde{\mathbf{X}}(t)$  such that the estimate  $\mathbf{X}(t)$  is close to  $\tilde{\mathbf{X}}(t)$  until  $t \geq T$ , i.e.,*

$$\|\mathbf{X}(t) - \tilde{\mathbf{X}}(t)\|_F < \epsilon_{app} \quad (17)$$

*for all  $t \in [0, T]$ .*

*Proof sketch (for detailed proof see Appendix C.1).* We prove this by first constructing a reference rank- $K$

trajectory,  $\tilde{\mathbf{X}}(t)$ , and then showing that the estimated trajectory,  $\mathbf{X}(t)$ , remains close to the reference rank- $K$  trajectory for a sufficiently small initialization as defined in (16). The parameters of the estimated trajectory are initialized uniformly and balanced, i.e.,  $\mathbf{g}(0) = \alpha_g \mathbf{1}_L$  and  $\mathbf{V}(0) = \alpha_V \mathbf{1}_{N \times L}$ . To construct the reference rank- $K$  trajectory,  $\tilde{\mathbf{X}}(t)$ , we begin by defining its own parameters  $(\tilde{\mathbf{g}}(t), \tilde{\mathbf{V}}(t))$ , such that  $\tilde{\mathbf{X}}(t) = (\tilde{\mathbf{g}}(t) \odot^2 \mathbf{1}_L) \odot \tilde{\mathbf{V}}(t)$ . The dynamics of these parameters are governed by the gradient flow on the loss function  $\mathcal{L}(\tilde{\mathbf{g}}(t), \tilde{\mathbf{V}}(t))$ . Crucially, for any support set  $\mathcal{S}_K$ , the corresponding parameters are initialized as, for  $i \in [N]$ ,

$$\tilde{g}_i(0) = \begin{cases} \sqrt{2}\rho^{1/3} & \forall i \in \mathcal{S}_K \\ 0 & \forall i \notin \mathcal{S}_K \end{cases}, \quad (18)$$

and

$$\tilde{V}_{ij}(0) = \begin{cases} \frac{1}{\sqrt{L}}\rho^{1/3} & \forall i \in \mathcal{S}_K, \forall j \in [L], \\ 0 & \forall i \notin \mathcal{S}_K \end{cases}, \quad (19)$$

where,  $\rho < L^{3/2}\alpha_V^3$  is a small positive scalar. Because these non-support rows for reference trajectory start at zero, Lemma 5.1 and Corollary 5.4, ensure they remain zero for all time  $t \geq 0$ . This construction guarantees the existence of a  $\tilde{\mathbf{X}}(t)$ , which is at most rank- $K$  matrix throughout its evolution. Note that this construction is purely for this theoretical proof; the proposed algorithm does not assume any knowledge of the support set or sparsity. To bound the distance between  $\mathbf{X}(t)$  and  $\tilde{\mathbf{X}}(t)$ , we analyze the divergence of their corresponding parameters using a Lyapunov function,  $\mathcal{E}(t) = \|(\mathbf{g}(t), \mathbf{V}(t)) - (\tilde{\mathbf{g}}(t), \tilde{\mathbf{V}}(t))\|^2$ . This allows practical initialization scale as is apparent in Equation (16). This stands in contrast to standard analysis techniques that rely on Grönwall's inequality (Razin et al., 2021; Gidel et al., 2019), which will lead to an initialization upper bound which will be exponentially smaller in  $T$  (i.e.,  $\exp(-\beta T)$ , where  $\beta$  is the smoothness constant).

The Lyapunov function is decomposed into three components: the energy of the estimated parameters, the energy of reference parameters and the corresponding cross term. The time derivative of each term is then upper bounded with a time-integrable growth. Integrating these bounds yields a rational polynomial-in-time bound on the Lyapunov function, ensuring that the parameter distance remains below a prescribed threshold for all  $t \in [0, T]$  provided the initialization satisfies (16).

Finally, the closeness of the parameter trajectories is translated to the distance between the trajectories  $\mathbf{X}(t)$  and  $\tilde{\mathbf{X}}(t)$  by applying the bound from Lemma 5.5. This leads to the theorem's main guarantee: for a sufficiently small initialization  $\alpha_V, \alpha_g$ , the estimated solution  $\mathbf{X}(t)$  is guaranteed to remain within a user-defined distance  $\epsilon_{\text{app}}$  of the reference row-sparse trajectory  $\tilde{\mathbf{X}}(t)$  for a specified time duration.  $\square$

This theorem provides the theoretical guarantee for the proposed framework. It formalizes the implicit regularization effect by establishing that with a sufficiently small and balanced initialization, the algorithm's estimated trajectory,  $\mathbf{X}(t)$  is guaranteed to stay within a predefined error ( $\epsilon_{\text{app}}$ ) of a reference rank- $K$  trajectory,  $\tilde{\mathbf{X}}(t)$ . By starting near the origin, the dynamics ensure that only a few rows that happen to have a slightly larger initial correlation with the true signal are selected to grow rapidly. Meanwhile balanced initialization ensures the proportional evolution of the factors required for the momentum-like dynamics to guide the algorithm's trajectory toward the row-sparse solution.

The following corollary extends the theoretical guarantees of Theorem 5.6. It establishes that if all reference trajectories converges uniformly to a global minimum of the objective function, then the estimated trajectory produced by the gradient flow of our proposed overparameterization will likewise converge to that same solution.

**Corollary 5.7.** *Assume the conditions of Theorem 5.6 and in addition, assume that all reference trajectories  $\tilde{\mathbf{X}}(t)$  converge to a solution  $\mathbf{X}^* \in \mathbb{R}^{N \times L}$  and this convergence is uniform in the sense that the trajectories are confined to a bounded domain, and for any  $\epsilon_{\text{app}} > 0$  there exists a time  $T_c \leq T$  after which they are all within a distance  $\epsilon_{\text{app}}$  from  $\mathbf{X}^*$ . Then for any  $\epsilon_{\text{app}} > 0$ , if the initialization scales  $\alpha_V, \alpha_g$  are sufficiently small, for any time  $t \in [T_c, T]$  it holds that  $\|\mathbf{X}(t) - \mathbf{X}^*\|_F \leq 2\epsilon_{\text{app}}$ .*

*Proof sketch (for detailed proof see Appendix C.3).* We assume that all reference trajectories  $\tilde{\mathbf{X}}(t)$  converge to the oracle solution  $\mathbf{X}^*$  within a finite time  $T > 0$ . This means that for any desired approximation error  $\epsilon_{\text{app}} > 0$  we have  $\|\tilde{\mathbf{X}}(t) - \mathbf{X}^*\| \leq \epsilon_{\text{app}}$ .

From Theorem 5.6, if the initialization values  $\alpha_V, \alpha_g$  are sufficiently small, the estimated trajectory is guaranteed to be within a distance of  $\epsilon_{\text{app}}$  from the reference trajectory at least until time  $T$ . This is a conditional guarantee that holds as long as both trajectories remain within a bounded domain. We show that the estimated trajectory  $\mathbf{X}(t)$  is also confined to a bounded domain. We know from our assumptions that the reference trajectory  $\tilde{\mathbf{X}}(t)$  is bounded. The result follows from applying the triangle inequality.  $\square$

## 6. Simulation

In this section, we present simulations to reinforce our theoretical results. We also compare the performance of our proposed IR-MMV approach against five established MMV recovery algorithms: M-OMP, M-SP, AMP-MMV, M-BSBL and M-FOCUSS. Unless otherwise specified, the default values for simulation parameters are:  $M = 500$ ,  $N = 10000$ ,  $L = 20$ , row sparsity level  $K = 3$  ( $K < N$ ) typically used

in IR/MMV literature. The sensing matrix  $\mathbf{A}$  is generated by drawing its entries from an i.i.d. sub-Gaussian distribution (to satisfy  $\mu$ -coherence property) with  $\ell_2$ -normalized columns. In line with our theoretical analysis, the algorithm's hyperparameters are configured as follows:  $\mathbf{g}$  is initialized with  $\alpha_V = 5 \times 10^{-4}$  to satisfy the small initialization requirement of Theorem 5.6, while the component matrix  $\mathbf{V}$  is initialized to  $\alpha_V = \frac{1}{\sqrt{2L}}\alpha_g$  to ensure the perfect row-wise balancedness. Finally, the maximum number of iterations is set to  $T = 5 \times 10^6$  to provide the algorithm with sufficient time to converge from its deliberately small initial state. For our experiments, the parameters of M-FOCUSS are set to  $p = 0.8$  and  $\lambda = 0.01$  as recommended by Cotter et al. (2005). Additionally, the exact sparsity level  $K$  was provided to M-OMP, M-SP and AMP-MMV, with the latter also receiving the true noise variance.

### 6.1. Balancedness and Incremental Learning

For this experiment, the ground truth MMV,  $\mathbf{X}$ , is constructed such that its active rows are set to constant values of  $\mathbf{1}_L, 2 \cdot \mathbf{1}_L$  and  $3 \cdot \mathbf{1}_L$ . Recall that the parameters are initialized to ensure perfect row-wise balancedness. The learning rates for the gradient descent updates for  $\mathbf{g}$  (i.e.,  $\eta_g$ ) and  $\mathbf{V}$  (i.e.,  $\eta_v$ ) are both set to  $10^{-4}$ , a small, constant value chosen for stable gradient descent. As illustrated in Figure 1, the evolution of  $\frac{1}{2}g_i^2(t)$  and  $\|\mathbf{V}_{i:}(t)\|_2^2$  is tracked throughout the optimization process. The empirical result support the theoretical findings of Lemma 5.1, by demonstrating that this balance is preserved over time. Note that the difference between the scalar component  $g_i$  and the row norm  $\|\mathbf{V}_{i:}\|_2$  does not grow confirms that the selected learning rate is sufficiently small. This validates the equivalence between our gradient descent implementation and the gradient flow dynamics assumed in our analysis.

This dynamic leads to a momentum-like effect and an incremental learning phenomenon, where rows of the MMV are learned one at a time, a behavior consistent with prior findings by Gissin et al. (2019); Razin et al. (2021); Hariz et al. (2024) in the context of implicit regularization via overparametrization. The magnitude of the row norms directly influences the learning speed, with smaller norms evolving more slowly and larger norms changing more rapidly. This dynamic implicitly promotes structured sparsity. The time-invariant balancedness property (Lemma 5.1) guarantees that if an element  $g_i(t)$  approaches zero, the corresponding row  $\mathbf{V}_{i:}$  will also converge to zero, rendering the entire  $i$ -th row of  $\mathbf{X}$  sparse.

### 6.2. Performance Comparison with Other Algorithms

The empirical performance of IR-MMV is compared against established MMV reconstruction algorithms, including M-OMP, M-SP, AMP-MMV, M-BSBL and M-FOCUSS. We

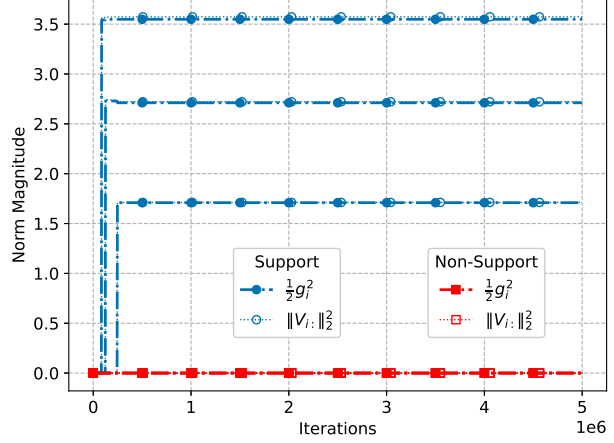


Figure 1. Evolution of the norms of the components for rows in the support and non-support sets

evaluate recovery using two metrics: the reconstruction accuracy, measured by the relative root mean squared error,  $\text{RMSE} = \frac{\|\mathbf{X} - \hat{\mathbf{X}}\|_F}{\|\mathbf{X}\|_F}$ , and the support recovery, quantified by the F1-Score  $\text{F1} = 2 \cdot \frac{\text{precision} \cdot \text{recall}}{\text{precision} + \text{recall}}$ . The values are averaged over 10 trials. In all experimental cases, the measurement matrix  $\mathbf{Y}$  is generated by adding noise to the signal according to the model  $\mathbf{Y} = \mathbf{AX} + \mathbf{W}$ . Consistent with IR literature, we construct the ground truth MMV,  $\mathbf{X}$ , such that its active rows are set to constant values of  $\mathbf{1}_L$ . We vary the Signal-to-Noise Ratio (SNR) while fixing the row-sparsity at  $K = 3$ . To further study the impact of signal complexity, we vary the sparsity level  $K$  with the SNR fixed at 4dB.

As seen in Figure 2, our approach consistently achieves performance comparable to the optimally tuned baselines. Our approach achieves this performance without any parameter tuning or prior knowledge of data-specific parameters. While M-BSBL does not require sparsity priors, they exhibit poor performance in the low SNR regime (0dB - 10dB). This is likely because, in these high-noise settings, reliably learning the hyperparameters from the data becomes infeasible. We also observe that the RMSE of M-FOCUSS remains consistently higher than that of the other approaches, even though its F1 score is 1.

The performance of M-OMP, M-SP, M-FOCUSS, and AMP-MMV drops when we introduce parameter mismatches (e.g.,  $K \pm 1$ ,  $\lambda \pm 10\%$  and  $\pm 10\%$  deviation in noise variance). As observed in Figures 2b, 2d, the greedy methods (M-OMP, M-SP) perform very poorly when the sparsity level is underestimated ( $K = 1$ ), failing to converge even at high SNR. When the sparsity is overestimated ( $K = 1$ ), the performance deteriorates, though the degradation is less severe compared to the underestimation case. In contrast, overestimation yields better error rates but prevents these algorithms from achieving perfect support recovery,

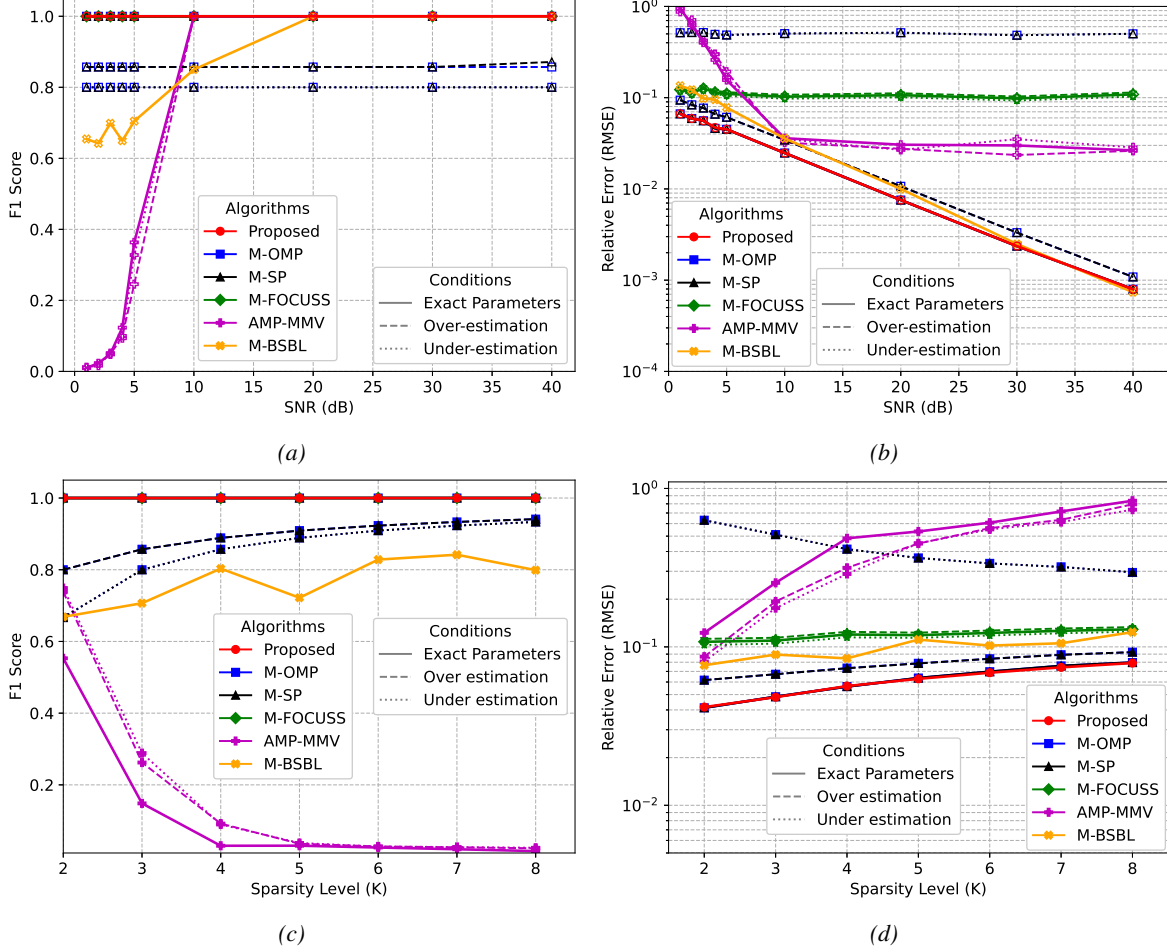


Figure 2. Performance comparison of the proposed IR-MMV approach against baseline algorithms with both optimal and mismatched parameters. (a) Support Recovery (F1-Score) vs. SNR (b) Relative Error (RMSE) vs. SNR, (c) Support Recovery (F1-Score) vs. Sparsity (K) and (d) Relative Error (RMSE) vs. Sparsity (K).

with F1-scores saturating below 1 (Figures 2a, 2c). We defer the results on MNIST data to Appendix D.

Summarizing, methods such as M-OMP, M-SP, M-FOCUSS, and AMP-MMV degrade in the presence of parameter misspecification while our method does not. Furthermore, we also outperform Bayesian approaches like M-BSBL at low SNR. Hence, our approach has significant utility in practical scenarios where typically there is parameter misspecification and/or low SNR.

## 7. Conclusion

We introduce a novel overparameterized factorization based on the Hadamard product to induce IR for structured sparse recovery of MMV. We show that the optimization dynamics naturally induce an implicit bias toward row-sparse solutions. Our characterization of the row norm dynamics identifies a momentum-like effect, where rows with larger norms

grow significantly faster than those with smaller norms, leading to an incremental learning process that provably favors low-rank solutions. We prove that the relative scaling between the parameters is preserved both globally and for each row throughout the optimization process. Furthermore, by employing a Lyapunov-based analysis of the gradient flow, we derive a formal convergence guarantee showing that with a sufficiently small and balanced initialization, the algorithm's trajectory remains close to an idealized row-sparse solution. We demonstrate that the proposed method achieves performance comparable to algorithms like M-OMP, M-SP, AMP-MMV and M-FOCUSS when they are provided with exact parameters. Moreover, our framework significantly outperforms these baselines in scenarios where they suffer from parameter mismatch, and maintains robust recovery even in low SNR regimes where M-BSBL performs poorly. Critically, the performance of the proposed framework is achieved without requiring prior knowledge of the sparsity level of the signal or its noise variance.

## Impact Statement

This paper presents work whose goal is to advance the field of Machine Learning. There are many potential societal consequences of our work, none which we feel must be specifically highlighted here.

## References

Arora, S., Cohen, N., and Hazan, E. On the optimization of deep networks: Implicit acceleration by overparameterization. In *International conference on machine learning*, pp. 244–253. PMLR, 2018.

Arora, S., Cohen, N., Hu, W., and Luo, Y. Implicit regularization in deep matrix factorization. *Advances in Neural Information Processing Systems*, 32, 2019.

Belitskii, G. et al. *Matrix norms and their applications*, volume 36. Birkhäuser, 2013.

Chen, D., Tian, L., and Xu, C. MMV-based OMP for DOA estimation with 1-bit measurement. In *Journal of Physics: Conference Series*, volume 1550, pp. 032150. IOP Publishing, 2020.

Chen, Z., Xiang, J., Bagnaninchi, P.-O., and Yang, Y. MMV-Net: A multiple measurement vector network for multi-frequency electrical impedance tomography. *IEEE Transactions on Neural Networks and Learning Systems*, 34(11):8938–8949, 2022.

Chou, H.-H., Maly, J., and Rauhut, H. More is less: inducing sparsity via overparameterization. *Information and Inference: A Journal of the IMA*, 12(3):1437–1460, 2023.

Cotter, S. F., Rao, B. D., Engan, K., and Kreutz-Delgado, K. Sparse solutions to linear inverse problems with multiple measurement vectors. *IEEE Transactions on signal processing*, 53(7):2477–2488, 2005.

Gidel, G., Bach, F., and Lacoste-Julien, S. Implicit regularization of discrete gradient dynamics in linear neural networks. *Advances in Neural Information Processing Systems*, 32, 2019.

Gissin, D., Shalev-Shwartz, S., and Daniely, A. The implicit bias of depth: How incremental learning drives generalization. *arXiv preprint arXiv:1909.12051*, 2019.

Gunasekar, S., Woodworth, B. E., Bhojanapalli, S., Neyshabur, B., and Srebro, N. Implicit regularization in matrix factorization. *Advances in neural information processing systems*, 30, 2017.

Hariz, K., Kadri, H., Ayache, S., Moakher, M., and Artières, T. Implicit regularization in deep tucker factorization: Low-rankness via structured sparsity. In *International Conference on Artificial Intelligence and Statistics*, pp. 2359–2367. PMLR, 2024.

Ji, Z. and Telgarsky, M. Gradient descent aligns the layers of deep linear networks. In *7th International Conference on Learning Representations, ICLR 2019*, 2019.

Li, J., Nguyen, T., Hegde, C., and Wong, K. W. Implicit sparse regularization: The impact of depth and early stopping. *Advances in Neural Information Processing Systems*, 34:28298–28309, 2021.

Li, J., Nguyen, T. V., Hegde, C., and Wong, R. K. Implicit regularization for group sparsity. *arXiv preprint arXiv:2301.12540*, 2023.

Li, Y., Ma, T., and Zhang, H. Algorithmic regularization in over-parameterized matrix sensing and neural networks with quadratic activations. In *Conference On Learning Theory*, pp. 2–47. PMLR, 2018.

Liu, B., Zhang, Z., Fan, H., and Fu, Q. Compression via compressive sensing: A low-power framework for the telemonitoring of multi-channel physiological signals. In *2013 IEEE International Conference on Bioinformatics and Biomedicine*, pp. 9–12. IEEE, 2013.

Liu, S., Zheng, L., Liu, L., and Lin, Q. MMV subspace pursuit (M-SP) algorithm for joint sparse multiple measurement vectors recovery. In *2019 IEEE 13th International Conference on ASIC (ASICON)*, pp. 1–4. IEEE, 2019.

Razin, N., Maman, A., and Cohen, N. Implicit regularization in tensor factorization. *Proceedings of Machine Learning Research*, 139:8913–8924, 2021. ISSN 26403498.

Soltanolkotabi, M., Stöger, D., and Xie, C. Implicit balancing and regularization: Generalization and convergence guarantees for overparameterized asymmetric matrix sensing. In *The Thirty Sixth Annual Conference on Learning Theory*, pp. 5140–5142. PMLR, 2023.

Teschl, G. *Ordinary differential equations and dynamical systems*, volume 140. American Mathematical Soc., 2012.

Vaskevicius, T., Kanade, V., and Rebeschini, P. Implicit regularization for optimal sparse recovery. *Advances in Neural Information Processing Systems*, 32, 2019.

Wu, X., Dobriban, E., Ren, T., Wu, S., Li, Z., Gunasekar, S., Ward, R., and Liu, Q. Implicit regularization and convergence for weight normalization. *Advances in Neural Information Processing Systems*, 33:2835–2847, 2020.

Yang, D. and Li, H. MMV-Net: A multiple measurement vector network for MIMO channel estimation. In *2024*

9th International Conference on Computer and Communication Systems (ICCCS), pp. 1027–1032. IEEE, 2024.

Zhang, X., Xie, L., and Wang, J. Some results on OMP algorithm for MMV problem. *Mathematical Methods in the Applied Sciences*, 45(9), 2022.

Zhao, P., Yang, Y., and He, Q.-C. High-dimensional linear regression via implicit regularization. *Biometrika*, 109 (4):1033–1046, 2022.

Ziniel, J. and Schniter, P. Efficient high-dimensional inference in the multiple measurement vector problem. *IEEE Transactions on Signal Processing*, 61(2):340–354, 2012.

## A. Gradient Updates

This section details the derivation of the gradient descent update rules for the parameters  $\mathbf{g}(t)$  and  $\mathbf{V}(t)$ . We consider the loss function for the proposed parameterization,  $\mathbf{X}(t) = \mathbf{g}^{\odot 2}(t)\mathbf{1}_L \odot \mathbf{V}(t)$ , which is reproduced here for readability:

$$\mathcal{L}(\mathbf{g}(t), \mathbf{V}(t)) = \|\mathbf{Y} - \mathbf{A}(\mathbf{g}^{\odot 2}(t)\mathbf{1}_L \odot \mathbf{V}(t))\|_F^2. \quad (20)$$

Let  $\mathbf{\Lambda} := \mathbf{A}^\top (\mathbf{Y} - \mathbf{A}\mathbf{X}(t))$ . We begin by deriving the partial derivative of the loss function  $\mathcal{L}(\mathbf{g}(t), \mathbf{V}(t))$  with respect to a single element  $g_l(t)$  (the  $l$ -th element of  $\mathbf{g}(t)$ ):

$$\nabla_{g_l(t)} \mathcal{L}(\mathbf{g}(t), \mathbf{V}(t)) = \nabla_{g_l(t)} \left( \sum_{i \in [M]} \sum_{j \in [L]} \left( Y_{ij} - \sum_{k \in [N]} A_{ik} g_k^2(t) V_{kj}(t) \right)^2 \right) \quad (21)$$

$$= -4 \sum_{i \in [M]} \sum_{j \in [L]} \left( Y_{ij} - \sum_{k \in [N]} A_{ik} g_k^2(t) V_{kj}(t) \right) A_{il} g_l(t) V_{lj}(t) \quad (22)$$

$$= -4g_l(t) \sum_{i \in [M]} \sum_{j \in [L]} A_{il} \left( Y_{ij} - \sum_{k \in [N]} A_{ik} g_k^2(t) V_{kj}(t) \right) V_{lj}(t) \quad (23)$$

$$= -4g_l(t) \sum_{j \in [L]} \mathbf{A}^\top (\mathbf{Y} - \mathbf{A}(\mathbf{g}^{\odot 2}(t)\mathbf{1}_L \odot \mathbf{V}(t)))_{lj} V_{lj}(t) \quad (24)$$

$$= -4g_l(t) \sum_{j \in [L]} \Lambda_{lj}(t) V_{lj}(t). \quad (25)$$

In vector form, the gradient with respect to  $\mathbf{g}$  is given by:

$$\nabla_{\mathbf{g}(t)} \mathcal{L}(\mathbf{g}(t), \mathbf{V}(t)) = -4\mathbf{g}(t) \odot ((\mathbf{\Lambda}(t) \odot \mathbf{V}(t))\mathbf{1}_L^\top). \quad (26)$$

Similarly, we compute the gradient of the loss function with respect to the element  $V_{lm}(t)$  (the  $(l, m)$ -th element of  $\mathbf{V}(t)$ ):

$$\nabla_{V_{lm}(t)} \mathcal{L}(\mathbf{g}(t), \mathbf{V}(t)) = \nabla_{V_{lm}(t)} \sum_{i \in [M]} \sum_j \left( Y_{ij} - \sum_{k \in [N]} A_{ik} g_k^2(t) V_{kj}(t) \right)^2 \quad (27)$$

$$= -2 \sum_{i \in [M]} \left( Y_{im} - \sum_{k \in [N]} A_{ik} g_k^2(t) V_{km}(t) \right) A_{il} g_l^2(t) \quad (28)$$

$$= -2g_l^2(t) \sum_{i \in [M]} A_{il} \left( Y_{im} - \sum_{k \in [N]} A_{ik} g_k^2(t) V_{km}(t) \right) \quad (29)$$

$$= -2g_l^2(t) (\mathbf{A}^\top (\mathbf{Y} - \mathbf{A}(\mathbf{g}^{\odot 2}(t)\mathbf{1}_L \odot \mathbf{V}(t)))_{lm} \quad (30)$$

$$= -2g_l^2(t) \Lambda_{lm}(t). \quad (31)$$

In matrix form this can be written as:

$$\nabla_{\mathbf{V}(t)} \mathcal{L}(\mathbf{g}(t), \mathbf{V}(t)) = -2\mathbf{g}^{\odot 2}(t)\mathbf{1}_L \odot \mathbf{\Lambda}(t) \quad (32)$$

## B. Characterization of the gradient flow

This section provides the lemmas and proofs that characterize the behavior of the system under the continuous gradient flow. In the following lemma, we establish a key ‘‘balancedness’’ property that is conserved by the gradient flow dynamics. Throughout this work, we denote the  $i$ -th row of any matrix  $\mathbf{Z}$  as  $\mathbf{Z}_{i:}$  and let  $\mathbf{1}_{N \times L}$  denote a matrix of ones of size  $N \times L$ .

**Lemma B.1** (Lemma 5.1 restated). *For the system evolving under continuous gradient flow for the set of update equations (4), (5) and (6), derived from the loss function  $\mathcal{L}(\mathbf{g}(t), \mathbf{V}(t)) = \|\mathbf{Y} - \mathbf{A}(\mathbf{g}(t)^{\odot 2}\mathbf{1}_L \odot \mathbf{V}(t))\|_F^2$ , the following properties hold for any time  $t \geq 0$ :*

1. *Global balancedness:* The quantity  $\frac{1}{2} \|\mathbf{g}(t)\|_2^2 - \|\mathbf{V}(t)\|_F^2$  is conserved throughout the optimization process:

$$\frac{1}{2} \|\mathbf{g}(t)\|_2^2 - \|\mathbf{V}(t)\|_F^2 = \frac{1}{2} \|\mathbf{g}(0)\|_2^2 - \|\mathbf{V}(0)\|_F^2$$

2. *Row-wise balancedness:* For each individual row  $i \in [N]$ , the quantity  $\frac{1}{2} g_i^2(t) - \sum_{j \in [L]} V_{ij}^2(t)$  is also conserved:

$$\frac{1}{2} g_i^2(t) - \sum_{j \in [L]} V_{ij}^2(t) = \frac{1}{2} g_i^2(0) - \sum_{j \in [L]} V_{ij}^2(0)$$

*Proof.* Let  $\Lambda(t) := \mathbf{A}^\top (\mathbf{Y} - \mathbf{A}(\mathbf{g}^{\odot 2}(t) \mathbf{1}_L \odot \mathbf{V}(t)))$ . Gradient flow is related to gradient as follows:

$$\frac{d}{dt} g_l(t) = -\nabla_{g_l} \mathcal{L}(\mathbf{g}(t), \mathbf{V}(t)). \quad (33)$$

From (25),

$$\frac{d}{dt} g_l(t) = 4g_l(t) \sum_{j \in [L]} \Lambda_{lj}(t) V_{lj}(t). \quad (34)$$

Similarly, from (31),

$$\frac{d}{dt} V_{lm}(t) = -\nabla_{V_{lm}} \mathcal{L}(\mathbf{g}(t), \mathbf{V}(t)), \quad (35)$$

$$= 2g_l^2(t) \Lambda_{lm}(t). \quad (36)$$

$$\frac{d}{dt} \|\mathbf{V}_{l:}(t)\|_2^2 = \frac{d}{dt} \left( \sum_{m \in [L]} V_{lm}^2(t) \right) = \sum_{m \in [L]} \frac{d}{dt} V_{lm}^2(t) \quad (37)$$

$$= 2 \sum_{m \in [L]} V_{lm}(t) \frac{d}{dt} V_{lm}(t). \quad (38)$$

Substituting (36)

$$\frac{d}{dt} \|\mathbf{V}_{l:}(t)\|_2^2 = 4g_l^2(t) \sum_{m \in [L]} V_{lm}(t) \Lambda_{lm}(t). \quad (39)$$

From (34) and (39),

$$g_l(t) \frac{d}{dt} g_l(t) = \frac{d}{dt} \|\mathbf{V}_{l:}(t)\|_2^2 \quad (40)$$

$$\frac{1}{2} \frac{d}{dt} g_l^2(t) = \frac{d}{dt} \|\mathbf{V}_{l:}(t)\|_2^2 \quad (41)$$

$$\frac{1}{2} \sum_{l \in [N]} \frac{d}{dt} g_l^2(t) = \sum_{l \in [N]} \frac{d}{dt} \|\mathbf{V}_{l:}(t)\|_2^2 \quad (42)$$

$$\frac{1}{2} \frac{d}{dt} \|\mathbf{g}(t)\|_2^2 = \frac{d}{dt} \|\mathbf{V}(t)\|_F^2. \quad (43)$$

Here,  $\mathbf{V}_{l:}(t)$  is the  $l$ -th row of matrix  $\mathbf{V}(t)$ . Integrating both sides of Equation (43) with respect to  $t$  from 0 to  $t$  directly yields the relationship:

$$\frac{1}{2} (\|\mathbf{g}(t)\|_2^2 - \|\mathbf{g}(0)\|_2^2) = \|\mathbf{V}(t)\|_F^2 - \|\mathbf{V}(0)\|_F^2. \quad (44)$$

Rearranging we get that

$$\frac{1}{2} \|\mathbf{g}(t)\|_2^2 - \|\mathbf{V}(t)\|_F^2 = \frac{1}{2} \|\mathbf{g}(0)\|_2^2 - \|\mathbf{V}(0)\|_F^2. \quad (45)$$

The second result follows from integrating both sides of (41) with respect to  $t$  from 0 to  $t$ .  $\square$

*Remark B.2* (Remark 5.2 restated). In the general case,  $\epsilon$  and  $\epsilon_r$  are independent quantities. However, under the specific initialization of Algorithm 1 (where  $g(0)$  and  $V(0)$  are initialized with constant values  $\alpha_g$  and  $\alpha_V$ ), it strictly holds that  $\epsilon_r \leq \epsilon$  for all  $t \geq 0$ .

*Proof.* Recall that the algorithm initializes the parameters as constants across all indices:  $g_i(0) = \alpha_g$  for all  $i \in [N]$  and  $V_{ij}(0) = \alpha_V$  for all  $i \in [N], j \in [L]$ .

Let  $e_i(t)$  denote the unbalancedness of the  $i$ -th row at time  $t$ :

$$e_i(t) = \frac{1}{2}g_i^2(t) - \sum_{j \in [L]} V_{ij}^2(t). \quad (46)$$

At initialization ( $t = 0$ ), we have:

$$e_i(0) = \frac{1}{2}\alpha_g^2 - L\alpha_V^2 = c, \quad \forall i \in [N], \quad (47)$$

where  $c$  is a constant scalar. Lemma B.1 demonstrates that this row-wise unbalancedness is conserved throughout the gradient flow. Therefore,  $e_i(t) = e_i(0) = c$  for all  $t \geq 0$ .

Substituting this into the definition of the global unbalancedness constant  $\epsilon$  (Definition 3.2), we obtain:

$$\epsilon(t) = \left| \sum_{i=1}^N e_i(t) \right| = \left| \sum_{i=1}^N c \right| = N|c|. \quad (48)$$

Similarly, for the row-unbalancedness constant  $\epsilon_r$  (Definition 3.3), we have:

$$\epsilon_r(t) = \max_{i \in [N]} |e_i(t)| = \max_{i \in [N]} |c| = |c|. \quad (49)$$

Comparing the two quantities, since  $N \geq 1$ :

$$\epsilon(t) = N\epsilon_r(t) \implies \epsilon_r(t) \leq \epsilon(t). \quad (50)$$

Finally, since these quantities are conserved throughout time, the time indexing ( $t$ ) can be dropped, yielding:

$$\epsilon_r \leq \epsilon. \quad (51)$$

□

**Lemma B.3.** For the system evolving under continuous gradient flow, as described in Lemma 5.1, with  $\Lambda(t) := \mathbf{A}^\top(\mathbf{Y} - \mathbf{A}(\mathbf{g}^{\odot 2}(t)\mathbf{1}_L \odot \mathbf{V}(t)))$  and any row  $l \in [N]$ , the following relationship hold for any time  $t \geq 0$ :

$$\frac{1}{2} \frac{d}{dt} g_l^2(t) = \sum_{j \in [L]} \frac{d}{dt} V_{lj}^2(t) = 4 \sum_{j \in [L]} (\Lambda(t) \odot \mathbf{X}(t))_{lj} = 4 (\Lambda(t) \mathbf{X}^\top(t))_{ll} \quad (52)$$

*Proof.*

From (39) and (41),

$$\frac{1}{2} \frac{d}{dt} g_l^2(t) = \frac{d}{dt} \|\mathbf{V}_{l:}(t)\|_2^2 = 4g_l^2(t) \sum_{j \in [L]} V_{lj}(t) \Lambda_{lj}(t) \quad (53)$$

$$= 4 \sum_{j \in [L]} \Lambda_{lj}(t) X_{lj}(t). \quad (54)$$

The last line follows from rearranging and substituting for  $X_{lj}(t) = g_l^2(t)V_{lj}(t)$  in (53).

In matrix form, equation (54) can be written as  $4 \sum_{j \in [L]} (\Lambda(t) \odot \mathbf{X}(t))_{lj}$  or  $4 (\Lambda(t) \mathbf{X}^\top(t))_{ll}$ . □

**Theorem B.4** (Theorem 5.3 restated). *For the system evolving under continuous gradient flow with updates as in (4), (5) and (6) with initialization  $g(0) = \alpha_g \mathbf{1}_L$  and  $V(0) = \alpha_V \mathbf{1}_{N \times L}$  where  $\alpha_g$  and  $\alpha_V$  are small positive scalars. Let  $\lambda_i(t)$  denote the  $i$ -th row of  $\Lambda(t)$ , and*

$$\hat{\mathbf{x}}_i(t) := \begin{cases} \frac{\mathbf{X}_{i:}(t)}{\|\mathbf{X}_{i:}(t)\|_2} & \text{if } \|\mathbf{X}_{i:}(t)\|_2 \neq 0 \\ \mathbf{0} & \text{if } \|\mathbf{X}_{i:}(t)\|_2 = 0 \end{cases}. \quad (55)$$

Then, for any time  $t \geq 0$  and for all  $i \in [N]$  where  $g_i^2(t) > 0$  and  $\sum_{m \in [N]} V_{im}^2(t) > 0$ , if  $\langle \lambda_i(t), \hat{\mathbf{x}}_i(t) \rangle \geq 0$ ,

$$\frac{d}{dt} \|\mathbf{X}_{i:}(t)\|_2 \leq 24 \langle \lambda_i(t), \hat{\mathbf{x}}_i(t) \rangle \left( \epsilon + \|\mathbf{X}_{i:}(t)\|_2^{2/3} \right)^2 \quad (56)$$

$$\frac{d}{dt} \|\mathbf{X}_{i:}(t)\|_2 \geq 6 \langle \lambda_i(t), \hat{\mathbf{x}}_i(t) \rangle \left( \frac{\|\mathbf{X}_{i:}(t)\|_2^2}{\epsilon + \|\mathbf{X}_{i:}(t)\|_2^{2/3}} \right), \quad (57)$$

if  $\langle \lambda_i(t), \hat{\mathbf{x}}_i(t) \rangle < 0$ ,

$$\frac{d}{dt} \|\mathbf{X}_{i:}(t)\|_2 \geq 24 \langle \lambda_i(t), \hat{\mathbf{x}}_i(t) \rangle \left( \epsilon + \|\mathbf{X}_{i:}(t)\|_2^{2/3} \right)^2 \quad (58)$$

$$\frac{d}{dt} \|\mathbf{X}_{i:}(t)\|_2 \leq 6 \langle \lambda_i(t), \hat{\mathbf{x}}_i(t) \rangle \left( \frac{\|\mathbf{X}_{i:}(t)\|_2^2}{\epsilon + \|\mathbf{X}_{i:}(t)\|_2^{2/3}} \right). \quad (59)$$

*Proof.* Note that

$$\langle \lambda_i(t), \hat{\mathbf{x}}_i(t) \rangle = \left( \Lambda(t) \frac{\mathbf{X}^\top(t)}{\|\mathbf{X}_{i:}(t)\|_2} \right)_{ii}. \quad (60)$$

With this identity established, we now derive the dynamics of the row norm  $\|\mathbf{X}_{i:}(t)\|_2$ :

$$\frac{d}{dt} \|\mathbf{X}_{i:}(t)\|_2 = \frac{1}{2\|\mathbf{X}_{i:}(t)\|_2} \frac{d}{dt} \left( \sum_j X_{ij}^2(t) \right). \quad (61)$$

Recall that  $X_{ij}(t) = g_i^2(t)V_{ij}(t)$ . Using Lemma B.3 and equation (34), we have

$$\frac{d}{dt} \sum_j X_{ij}^2(t) = 4g_i^4(t)(\Lambda(t)\mathbf{X}^\top(t))_{ii} + 16 \sum_{j \in [L]} V_{ij}^2(t)g_i^2(t) \sum_k \Lambda_{ik}(t)X_{ik}(t) \quad (62)$$

$$= 4 \left( g_i^4(t)(\Lambda(t)\mathbf{X}^\top(t))_{ii} + 4 \sum_{j \in [L]} V_{ij}^2(t)g_i^2(t)(\Lambda(t)\mathbf{X}^\top(t))_{ii} \right) \quad (63)$$

$$= 4(\Lambda(t)\mathbf{X}^\top(t))_{ii} \left( g_i^4(t) + 4 \sum_{j \in [L]} V_{ij}^2(t)g_i^2(t) \right) \quad (64)$$

Substituting equation (64) in (61),

$$\frac{d}{dt} \|\mathbf{X}_{i:}(t)\|_2 = \frac{2}{\|\mathbf{X}_{i:}(t)\|_2} (\Lambda(t)\mathbf{X}^\top(t))_{ii} \left( g_i^4(t) + 4 \sum_{j \in [L]} V_{ij}^2(t)g_i^2(t) \right) \quad (65)$$

$$\stackrel{a}{\leq} 24 \sum_{j \in [L]} \Lambda_{ij}(t) \frac{X_{ij}(t)}{\|\mathbf{X}_{i:}(t)\|_2} \left( \epsilon + \|\mathbf{X}_{i:}(t)\|_2^{2/3} \right)^2 \quad (66)$$

$$\leq 24 \langle \lambda_i(t), \hat{\mathbf{x}}_i(t) \rangle \left( \epsilon + \|\mathbf{X}_{i:}(t)\|_2^{2/3} \right)^2. \quad (67)$$

Note that in this case,  $\langle \boldsymbol{\lambda}_i(t), \hat{\mathbf{x}}(t)_i \rangle$  is non-negative. From the definition of unbalancedness, we have  $\left| \frac{1}{2}g_i^2(t) - \sum_{m \in [L]} V_{im}^2(t) \right| \leq \epsilon_r$ . The inequality in step (a) follows by substituting (60), (70) and (71) in (65).

$$\sum_{m \in [L]} V_{im}^2(t) \leq \epsilon_r + \min \left\{ \sum_{m \in [L]} V_{im}^2(t), \frac{1}{2}g_i^2(t), \frac{1}{2}g_i^2(t) \right\} \quad (68)$$

$$\leq \epsilon_r + \left( \frac{1}{4}g_i^4(t) \sum_{m \in [L]} V_{im}^2(t) \right)^{\frac{1}{3}}. \quad (69)$$

Recall that  $X_{im}(t) = g_i^2(t)V_{im}(t)$ :

$$\sum_{m \in [L]} V_{im}^2(t) \leq \epsilon + \|\mathbf{X}_{i:}(t)\|_2^{2/3}. \quad (70)$$

Similarly, we have:

$$\frac{1}{2}g_i^2(t) \leq \epsilon + \|\mathbf{X}_{i:}(t)\|_2^{2/3}. \quad (71)$$

For the lower bound, we start from (65) and rewrite the expression as follows:

$$\frac{d}{dt} \|\mathbf{X}_{i:}(t)\|_2 = \frac{2}{\|\mathbf{X}_{i:}(t)\|_2} (\boldsymbol{\Lambda}(t)\mathbf{X}^\top(t))_{ii} \left( g_i^4(t) + 4 \sum_{j \in [L]} V_{ij}^2(t)g_i^2(t) \right) \quad (72)$$

$$= \frac{2}{\|\mathbf{X}_{i:}(t)\|_2} (\boldsymbol{\Lambda}(t)\mathbf{X}^\top(t))_{ii} \left( \frac{g_i^4(t) \sum_{j \in [L]} V_{ij}^2(t)}{\sum_{j \in [L]} V_{ij}^2(t)} + 4 \frac{\sum_{j \in [L]} V_{ij}^2(t)g_i^4(t)}{g_i^2(t)} \right) \quad (73)$$

$$= \frac{2}{\|\mathbf{X}_{i:}(t)\|_2} (\boldsymbol{\Lambda}(t)\mathbf{X}^\top(t))_{ii} \sum_{j \in [L]} X_{ij}^2(t) \left( \frac{1}{\sum_{j \in [L]} V_{ij}^2(t)} + 2 \frac{1}{\frac{1}{2}g_i^2(t)} \right). \quad (74)$$

Substituting the inequalities (70) and (71),

$$\frac{d}{dt} \|\mathbf{X}_{i:}(t)\|_2 \geq 6 \langle \boldsymbol{\lambda}_i(t), \hat{\mathbf{x}}_i(t) \rangle \left( \frac{\|\mathbf{X}_{i:}(t)\|_2^2}{\epsilon + \|\mathbf{X}_{i:}(t)\|_2^{2/3}} \right). \quad (75)$$

When  $\langle \boldsymbol{\lambda}_i, \hat{\mathbf{x}}_i \rangle < 0$ , the direction of inequality in (66) and (75) reverses resulting in the second part of the lemma.  $\square$

Now, in the following lemma we look at a special case when  $\epsilon = 0$

**Corollary B.5** (Corollary 5.4 restated). *Assume that the system evolves under continuous gradient flow, as described in Lemma B.4, with perfect row balancedness (i.e.,  $\frac{1}{2}g_i^2(t) = \sum_j V_{ij}^2(t) \forall i \in [N]$  and time  $t \geq 0$ ). The rate of change of the Euclidean norm of the  $i$ -th row of  $\mathbf{X}(t)$  is characterized by:*

$$\frac{d}{dt} \|\mathbf{X}_{i:}(t)\|_2 = 2^{2/3} \cdot 6 \langle \boldsymbol{\lambda}_i(t), \hat{\mathbf{x}}_i(t) \rangle \|\mathbf{X}_{i:}(t)\|_2^{4/3} \quad (76)$$

*Proof.*

Rewriting (65),

$$\frac{d}{dt} \|\mathbf{X}_{i:}(t)\|_2 = \frac{2}{\|\mathbf{X}_{i:}(t)\|_2} (\boldsymbol{\Lambda}(t)\mathbf{X}^\top(t))_{ii} \left( g_i^4(t) + 4 \sum_{j \in [L]} V_{ij}^2(t)g_i^2(t) \right). \quad (77)$$

Substituting perfect-row balancedness condition  $\frac{1}{2}g_i^2(t) = \sum_{j \in [L]} V_{ij}^2(t)$ :

$$\frac{d}{dt} \|\mathbf{X}_{i:}(t)\|_2 = \frac{6}{\|\mathbf{X}_{i:}(t)\|_2} (\mathbf{\Lambda}(t) \mathbf{X}^\top(t))_{ii} g_i^4(t) \stackrel{a}{=} 2^{2/3} 6 \langle \mathbf{\lambda}_i(t), \hat{\mathbf{x}}_i(t) \rangle \|\mathbf{X}_{i:}(t)\|_2^{4/3}, \quad (78)$$

where equality (a) follows by substituting  $g_i^4(t) = 2^{2/3} \|\mathbf{X}_{i:}(t)\|_2^{4/3}$  since  $\|\mathbf{X}_{i:}(t)\|_2^2 = \frac{1}{2}g_i^6(t)$ , and recalling  $\langle \mathbf{\lambda}_i(t), \hat{\mathbf{x}}_i(t) \rangle = \frac{(\mathbf{\Lambda}(t) \mathbf{X}^\top(t))_{ii}}{\|\mathbf{X}_{i:}(t)\|_2}$ .

□

**Lemma B.6.** *For the system evolving under continuous gradient flow, the loss function  $\mathcal{L}(\mathbf{g}(t), \mathbf{V}(t)) = \|\mathbf{Y} - \mathbf{A}(\mathbf{g}(t) \odot^2 \mathbf{1}_L \odot \mathbf{V}(t))\|_F^2$  is locally Lipschitz continuous with respect to each component  $g_n(t)$  (for all  $n \in [N]$ ) and  $V_{nl}(t)$  (for all  $n \in [N], l \in [L]$ ) over a domain of interest  $\mathcal{D} := \{(g_n(t), V_{nl}(t)) \in \mathbb{R}^N \times \mathbb{R}^{N \times L} : |g_n(t)| \leq B_g, |V_{nl}(t)| \leq B_V \forall n \in [N], l \in [L]\}$  for some constants  $B_g > 0$  and  $B_V > 0$ . Furthermore,  $\mathcal{L}(\mathbf{g}(t), \mathbf{V}(t))$  is uniformly continuous with respect to time  $t$ .*

*Proof.* We begin by proving the local Lipschitz continuity of the loss function. This requires bounding the term  $\left| \mathcal{L}(\mathbf{g}(t), \mathbf{V}(t)) - \mathcal{L}(\tilde{\mathbf{g}}(t), \tilde{\mathbf{V}}(t)) \right|$  by the distance between the parameters  $(\tilde{\mathbf{g}}(t), \tilde{\mathbf{V}}(t))$  and  $(\mathbf{g}(t), \mathbf{V}(t))$ . Let the distance between the parameters at time  $t$  be defined as

$$\left\| (\tilde{\mathbf{g}}(t), \tilde{\mathbf{V}}(t)) - (\mathbf{g}(t), \mathbf{V}(t)) \right\|^2 = \sum_{j \in [L]} \sum_{k \in [N]} \left( (\tilde{V}_{kj}(t) - V_{kj}(t))^2 + (\tilde{g}_k(t) - g_k(t))^2 \right). \quad (79)$$

For brevity, we omit the explicit time dependency  $(t)$  for variables  $\mathbf{g}$ ,  $\mathbf{V}$ ,  $\mathbf{X}$ , and  $\mathbf{\Lambda}$  unless otherwise specified.

We now expand term  $\left| \mathcal{L}(\mathbf{g}, \mathbf{V}) - \mathcal{L}(\tilde{\mathbf{g}}, \tilde{\mathbf{V}}) \right|$ :

$$\left| \mathcal{L}(\mathbf{g}, \mathbf{V}) - \mathcal{L}(\tilde{\mathbf{g}}, \tilde{\mathbf{V}}) \right| = \left| \sum_{i \in [M]} \sum_{j \in [L]} \left( Y_{ij} - \sum_{k \in [N]} A_{ik} g_k^2 V_{kj} \right)^2 - \sum_{i \in [M]} \sum_{j \in [L]} \left( Y_{ij} - \sum_{k \in [N]} A_{ik} \tilde{g}_k^2 \tilde{V}_{kj} \right)^2 \right| \quad (80)$$

$$\leq \sum_{i \in [M]} \sum_{j \in [L]} \left| \left( \sum_{k \in [N]} A_{ik} (\tilde{g}_k^2 \tilde{V}_{kj} - g_k^2 V_{kj}) \right) \left( 2Y_{ij} - \sum_{k \in [N]} A_{ik} (g_k^2 V_{kj} + \tilde{g}_k^2 \tilde{V}_{kj}) \right) \right| \quad (81)$$

$$\leq 2C_1 \sum_{i \in [M]} \sum_{j \in [L]} \left| \sum_{k \in [N]} (\tilde{g}_k^2 \tilde{V}_{kj} - g_k^2 V_{kj}) \right|, \quad (82)$$

where  $C_1 = B_Y + N\mu B_g^2 B_V$ . Last line follows by noting that  $g_i, V_{ij} \in \mathcal{D}$ , and that  $\mathbf{A}$  is  $\mu$ -coherent with  $\ell_2$ -normalized columns i.e.,  $\left| \sum_{b \in [M]} A_{bn} A_{bc} \right| \leq \mu \leq 1$ . Let  $B_Y = \max_{i,j} \{Y_{ij}\}$ :

$$\left| \tilde{g}_k^2 \tilde{V}_{kj} - g_k^2 V_{kj} \right| = \left| \tilde{g}_k^2 \tilde{V}_{kj} - \tilde{g}_k^2 V_{kj} + \tilde{g}_k^2 V_{kj} - g_k^2 V_{kj} \right| \quad (83)$$

$$= \left| \tilde{g}_k^2 (\tilde{V}_{kj} - V_{kj}) + V_{kj} (\tilde{g}_k^2 - g_k^2) \right|. \quad (84)$$

Substituting the parameter bounds from the domain  $\mathcal{D}$

$$\leq B_g^2 \left| \tilde{V}_{kj} - V_{kj} \right| + 2B_V B_g |\tilde{g}_k - g_k| \quad (85)$$

$$\leq C_2 \left( \left| \tilde{V}_{kj} - V_{kj} \right| + |\tilde{g}_k - g_k| \right). \quad (86)$$

where  $C_2 = \max \{1, B_g^2, 2B_V B_g\}$ . Substituting (86) back into (82), we can finally write:

$$\left| \mathcal{L}(\mathbf{g}, \mathbf{V}) - \mathcal{L}(\tilde{\mathbf{g}}, \tilde{\mathbf{V}}) \right| \leq 2C_1 C_2 M \sum_{j \in [L]} \sum_{k \in [N]} \left( |\tilde{V}_{kj} - V_{kj}| + |\tilde{g}_k - g_k| \right). \quad (87)$$

Using the norm equivalence  $\sum_{i=1}^M \sum_{j=1}^N |a_{ij}| \leq \sqrt{MN \sum_{i=1}^M \sum_{j=1}^N |a_{ij}|^2}$ :

$$\left| \mathcal{L}(\mathbf{g}, \mathbf{V}) - \mathcal{L}(\tilde{\mathbf{g}}, \tilde{\mathbf{V}}) \right| \leq 2C_1 C_2 M \sqrt{NL} \sqrt{\sum_{j \in [L]} \sum_{k \in [N]} \left( (\tilde{V}_{kj} - V_{kj})^2 + (\tilde{g}_k - g_k)^2 \right)} \quad (88)$$

$$\leq 2C_1 C_2 M \sqrt{NL} \left| (\tilde{\mathbf{g}}, \tilde{\mathbf{V}}) - (\mathbf{g}, \mathbf{V}) \right|. \quad (89)$$

Thus,  $\mathcal{L}(\mathbf{g}, \mathbf{V})$  is locally Lipschitz continuous with respect to  $g_l \forall l \in [N]$  and  $V_{lm} \forall l \in [N], m \in [L]$ . Now, we proceed to prove the uniform continuity of  $\mathcal{L}(\mathbf{g}(t), \mathbf{V}(t))$  with respect to  $t$ .

$$\frac{d}{dt} \mathcal{L}(\mathbf{g}(t), \mathbf{V}(t)) = \sum_{n \in [N]} \nabla_{g_n} \mathcal{L}(\mathbf{g}(t), \mathbf{V}(t)) \frac{d}{dt} g_n(t) + \sum_{n \in [N]} \sum_{l \in [L]} \nabla_{V_{nl}} \mathcal{L}(\mathbf{g}(t), \mathbf{V}(t)) \frac{d}{dt} V_{nl}(t). \quad (90)$$

By substituting the gradient flow relations  $\frac{d}{dt} g_i(t) = -\nabla_{g_i(t)} \mathcal{L}(\mathbf{g}(t), \mathbf{V}(t))$  and  $\frac{d}{dt} V_{il}(t) = -\nabla_{V_{il}(t)} \mathcal{L}(\mathbf{g}(t), \mathbf{V}(t))$ , this becomes:

$$\frac{d}{dt} \mathcal{L}(\mathbf{g}(t), \mathbf{V}(t)) = - \sum_{n \in [N]} (\nabla_{g_n} \mathcal{L}(\mathbf{g}(t), \mathbf{V}(t)))^2 - \sum_{n \in [N]} \sum_{l \in [L]} (\nabla_{V_{nl}} \mathcal{L}(\mathbf{g}(t), \mathbf{V}(t)))^2. \quad (91)$$

Substituting equation (25) and (31) in the above equation, we have:

$$\frac{d}{dt} \mathcal{L}(\mathbf{g}(t), \mathbf{V}(t)) = \sum_{n \in [N]} \left( \left( 4g_n(t) \sum_{l \in [L]} \Lambda_{nl}(t) V_{nl}(t) \right)^2 + \sum_{l \in [L]} 4g_n^4(t) \Lambda_{nl}^2(t) \right). \quad (92)$$

To complete the proof, we must show that the magnitude of this time derivative is bounded by a constant. First, we establish an upper bound for  $|\Lambda_{nl}(t)|$ :

$$|\Lambda_{nl}(t)| = |(\mathbf{A}^\top (\mathbf{Y} - \mathbf{AX}(t)))_{nl}| \quad (93)$$

$$= \left| \sum_{b \in [M]} \left( A_{bn} \left( Y_{bl} - \sum_{c \in [N]} A_{bc} X_{cl}(t) \right) \right) \right| \quad (94)$$

$$\leq \left| \sum_{b \in [M]} A_{bn} Y_{bl} \right| + \left| \sum_{b \in [M]} A_{bn} \sum_{c \in [N]} A_{bc} X_{cl}(t) \right|. \quad (95)$$

Using  $\mathbf{A}$  is  $\ell_2$ -normalized columns and  $X_{cl}(t) = g_c^2(t) V_{cl}(t)$ , we have:

$$|\Lambda_{nl}| \leq \left| \sum_{b \in [M]} A_{bn} Y_{bl} \right| + \sum_{c \in [N]} \left| \sum_{b \in [M]} A_{bn} A_{bc} \right| \left| g_c^2(t) V_{cl}(t) \right|. \quad (96)$$

Substituting the parameter bounds from the domain of interest  $\mathcal{D}$  in the above equation, we have:

$$|\Lambda_{nl}| \leq MB_Y + N\mu B_g^2 B_V \quad (97)$$

$$\leq M (B_Y + N\mu B_g^2 B_V). \quad (98)$$

Substituting this bound along with the parameter bounds from  $\mathcal{D}$  in (92), we obtain:

$$\left| \frac{d}{dt} \mathcal{L}(\mathbf{g}(t), \mathbf{V}(t)) \right| \leq \sum_n (16L^2 B_g^2 B_V^2 M^2 C_1^2 + 4LB_g^4 M^2 C_1^2) \quad (99)$$

$$\leq 4NM^2 LC_2^2 C_1^2 \left( L + \frac{1}{2} \right). \quad (100)$$

Since  $M, N, L, B_g, B_V, C_1, C_2$  are all finite constants, the entire expression is bounded by a constant. Thus,  $\mathcal{L}(\cdot, \cdot)$  is uniform with respect to  $t$ .  $\square$

**Lemma B.7.** *For the system evolving under continuous gradient flow, as described in Corollary B.5:*

**Case I:** If  $\frac{1}{\sqrt{2}}|g_i(0)| = \|V_{i:}(0)\| = 0$ , then  $\frac{1}{\sqrt{2}}\|g_i(t)\| = \|V_{i:}(t)\| = 0$  for all  $t > 0$ .

**Case II:** If  $\frac{1}{\sqrt{2}}|g_i(0)| = \|V_{i:}(0)\| > 0$ , then  $\frac{1}{\sqrt{2}}|g_i(t)| = \|V_{i:}(t)\| > 0$  for all  $t > 0$ .

*Proof.* **Case I:**  $\frac{1}{\sqrt{2}}|g_i(0)| = \|V_{i:}(0)\| = 0$ ; We also have  $V_{il}(0) = 0 \forall l \in [L]$ .

Recall that gradient flow is related to gradient as:

$$\frac{d}{dt} g_i(t) = -\nabla_{g_i(t)} \mathcal{L}(\mathbf{g}(t), \mathbf{V}(t)) = 4g_i \sum_j \Lambda_{ij} V_{ij},$$

and

$$\frac{d}{dt} V_{il}(t) = -\nabla_{V_{il}(t)} \mathcal{L}(\mathbf{g}(t), \mathbf{V}(t)) = 2g_i^2 \Lambda_{il}. \quad (101)$$

This system forms an initial value problem in both  $g_i(t)$  and  $V_{il}(t)$ . Because the loss function gradient is locally Lipschitz continuous with respect to the parameters  $(\mathbf{g}(t), \mathbf{V}(t))$  and uniformly continuous with respect to time  $t$ , Lemma B.6 and Teschl (2012, Theorem 2.2)<sup>1</sup>, guarantees a unique solution for  $g_i(t)$  and  $V_{il}(t)$ . At  $t = 0$ ,

$$\left. \frac{d}{dt} g_i(t) \right|_{t=0} = 0; \quad \left. \frac{d}{dt} V_{il}(t) \right|_{t=0} = 0. \quad (102)$$

The constant functions,  $g_i(t) = 0, V_{il}(t) = 0$  form a valid solution to the initial value problem. Since the solution is unique, this must be the only solution.

In our setting  $g_i(t)$  and  $V_{i:}(t)$  are continuous,  $\frac{1}{\sqrt{2}}|g_i(0)| = \|V_{i:}(0)\| > 0$ , and  $\langle \boldsymbol{\lambda}_i(t), \hat{\mathbf{x}}_i(t) \rangle$ , is bounded because parameters lie in bounded domain. To complete the proof, we now show that the differential equations governing these norms follow the format required by the cited lemma:

$$\frac{d}{dt} |g_i(t)| = \frac{1}{2|g_i(t)|} \frac{d}{dt} g_i^2(t); \quad \frac{d}{dt} \|V_{i:}(t)\| = \frac{1}{2\|V_{i:}\|} \frac{d}{dt} \|V_{i:}(t)\|^2. \quad (103)$$

Recalling the result from Lemma B.3, we have the dynamics of the norms in terms of  $(\mathbf{\Lambda} \mathbf{X}^\top)_{ii}$ . By applying the innerproduct identity (equation (60)), we have:

$$\frac{d}{dt} |g_i(t)| = \frac{4g_i^2(t) \|V_{i:}(t)\|}{|g_i(t)|} \langle \boldsymbol{\lambda}_i(t), \hat{\mathbf{x}}_i(t) \rangle. \quad (104)$$

<sup>1</sup>(Teschl, 2012, Theorem 2.2) (Picard-Lindelöf): Suppose  $f \in C(U, \mathbb{R}^n)$ , where  $U$  is an open subset of  $\mathbb{R}^{n+1}$ , and  $(t_0, x_0) \in U$ . If  $f$  is locally Lipschitz continuous in the second argument, uniformly with respect to the first, then there exists a unique local solution  $\bar{x}(t) \in C^1(I)$  of the initial value problem, where  $I$  is some interval around  $t_0$ .

Similarly, we have

$$\frac{d}{dt} \|V_{i:}(t)\| = 2 \frac{g_i^2(t) \|V_{i:}(t)\|}{\|V_{i:}(t)\|} \langle \boldsymbol{\lambda}_i(t), \hat{\mathbf{x}}_i(t) \rangle. \quad (105)$$

Applying the perfect row-balancedness condition (namely,  $\frac{1}{2}g_i^2(t) = \sum_j V_{ij}^2 = \|\mathbf{V}_{i:}(t)\|^2$ ) to equations (104) and (105) simplify to:

$$\frac{d}{dt} |g_i(t)| = 2\sqrt{2}g_i^2(t) \langle \boldsymbol{\lambda}_i(t), \hat{\mathbf{x}}_i(t) \rangle, \quad (106)$$

and

$$\frac{d}{dt} \|V_{i:}(t)\| = 4\|V_{i:}(t)\|^2 \langle \boldsymbol{\lambda}_i(t), \hat{\mathbf{x}}_i(t) \rangle. \quad (107)$$

As all the necessary conditions of Razin et al. (2021, Lemma 5) are met, we have  $g_i(t) > 0$ ,  $\|V_{i:}(t)\| > 0$ .  $\square$

Now that we have characterized the fundamental dynamics of the gradient flow, in the next section, we develop the essential theoretical tools needed to prove our main result.

## C. Supporting Lemmas and the Proof of the Theorem 5.6

We begin by defining the initialization schemes for both the estimated trajectory  $\mathbf{X}(t)$ , and some reference rank- $K$  trajectory  $\tilde{\mathbf{X}}(t)$ .

### INITIALIZATION OF ESTIMATED TRAJECTORY

At time  $t = 0$ , the parameters are initialized uniformly irrespective of the sparsity support  $\mathcal{S}_K$ , i.e.,

$$g_i(0) = \alpha_g; \quad V_{ij}(0) = \alpha_V \quad \forall i \in [N], j \in [L]. \quad (108)$$

To ensure perfect row-balancedness (i.e.,  $\frac{1}{2}g_i^2(t) = \sum_j V_{ij}^2(t)$ ), at  $t = 0$ , we keep  $\frac{1}{2}\alpha_g^2 = L\alpha_V^2$ . This initialization results in the following results, at  $t = 0$

$$X_{ij}(0) = g_i^2(0)V_{ij}(0) = \alpha_g^2\alpha_V = 2L\alpha_V^3 = \frac{1}{\sqrt{2L}}\alpha_g^3 \quad (109)$$

As a result the Euclidean norm of  $i$ -th row of the estimated trajectory at time  $t = 0$  is:

$$\|\mathbf{X}_{i:}(0)\|_2 = g_i^2(0)\|\mathbf{V}_{i:}(0)\|_2 = \alpha_g^2\sqrt{L}\alpha_V = \frac{1}{\sqrt{2}}\alpha_g^3 = 2L\sqrt{L}\alpha_V^3. \quad (110)$$

### INITIALIZATION OF THE REFERENCE TRAJECTORY

Next, we construct a reference rank- $K$  trajectory, denoted as  $\tilde{\mathbf{X}}(t)$ . For a given support set  $\mathcal{S}_K$ , we initialize its corresponding parameters so that the rows outside the support are zero:

$$\tilde{g}_i(0) = \begin{cases} \sqrt{2}\rho^{1/3} & \forall i \in \mathcal{S}_K \\ 0 & \forall i \notin \mathcal{S}_K \end{cases}; \quad \tilde{V}_{i,j}(0) = \begin{cases} \frac{1}{\sqrt{L}}\rho^{1/3} & \forall i \in \mathcal{S}_K, \forall j \in [N] \\ 0 & \forall i \notin \mathcal{S}_K \end{cases}. \quad (111)$$

Consequently, the initial row norms are given by

$$\|\tilde{\mathbf{V}}_{i:}(0)\|_2 = \begin{cases} \rho^{1/3} & \forall i \in \mathcal{S}_K \\ 0 & \forall i \notin \mathcal{S}_K \end{cases}. \quad (112)$$

Here  $\rho > 0$  is a very small positive constant. This construction ensures that the reference trajectory is perfectly row-balanced (i.e.,  $\frac{1}{2}g_i^2(t) = \sum_j V_{ij}^2$ ), at initialization and rank- $K$  at initialization. Note that since  $X_{ij}(t) = g_i^2(t)V_{ij}(t)$  the above initializations result in the following expression:

$$\|\tilde{\mathbf{X}}_{i:}(0)\|_2 = \begin{cases} 2\rho & \forall i \in \mathcal{S}_K, \\ 0 & \forall i \notin \mathcal{S}_K \end{cases} \quad (113)$$

Note that this construction is purely for this theoretical proof; the proposed algorithm does not assume any knowledge of the support set or sparsity.

With the initializations established, the following lemma formalizes the dynamics of the constructed reference rank- $K$  trajectory.

**Lemma C.1.** *Let a  $K$ -component system be defined by parameters  $\bar{\mathbf{g}}(t) \in \mathbb{R}^K$  and  $\bar{\mathbf{V}}(t) \in \mathbb{R}^{K \times L}$ . Let  $\mathcal{S}_K \subseteq [N]$  be a support set of size  $K = |\mathcal{S}_K| \leq N$ . Let us construct an  $N$ -component trajectory  $\tilde{\mathbf{g}}(t) \in \mathbb{R}^N$  and  $\tilde{\mathbf{V}}(t) \in \mathbb{R}^{N \times L}$  by embedding the  $K$ -component system into a larger  $N$ -dimensional space and padding the remaining components with zeros. To formally relate the  $K$ -component system to its  $N$ -component embedding, we create an ordered correspondence between the indices of the small system,  $\{1, \dots, K\}$ , and the ordered indices of the support set,  $\mathcal{S}_K = \{s_1, s_2, \dots, s_K\}$ . The embedding is then defined as:*

$$\tilde{g}_i(t) := \begin{cases} \bar{g}_k(t) & \text{if } i = s_k \text{ for } k \in [K] \\ 0 & \text{if } i \notin \mathcal{S}_K \end{cases} \quad (114)$$

$$\tilde{V}_{il}(t) := \begin{cases} \bar{V}_{kl}(t) & \text{if } i = s_k \text{ for } k \in [K] \\ 0 & \text{if } i \notin \mathcal{S}_K \end{cases} \quad (115)$$

Let  $\bar{\mathbf{A}}$  be the sub-matrix of  $\mathbf{A}$  such that  $\bar{\mathbf{A}}$  contains only columns of  $\mathbf{A}$  that correspond to the support indices  $\mathcal{S}_K$ . Let the dynamics of  $\bar{\mathbf{g}}(t)$  and  $\bar{\mathbf{V}}(t)$  be derived from the loss function  $\mathcal{L}_K(\bar{\mathbf{g}}(t), \bar{\mathbf{V}}(t)) = \|\mathbf{Y} - \bar{\mathbf{A}}(\bar{\mathbf{g}}(t)^{\odot 2} \mathbf{1}_L \odot \bar{\mathbf{V}}(t))\|_F^2$  where  $\bar{\mathbf{X}}(t) = (\bar{\mathbf{g}}(t)^{\odot 2} \mathbf{1}_L) \odot \bar{\mathbf{V}}(t)$  follow gradient flow path. Then, the dynamics of  $\tilde{\mathbf{g}}(t)$  and  $\tilde{\mathbf{V}}(t)$ , derived from the loss function  $\mathcal{L}_N(\tilde{\mathbf{g}}(t), \tilde{\mathbf{V}}(t)) = \|\mathbf{Y} - \mathbf{A}(\tilde{\mathbf{g}}(t)^{\odot 2} \mathbf{1}_L \odot \tilde{\mathbf{V}}(t))\|_F^2$  where  $\tilde{\mathbf{X}}(t) = (\tilde{\mathbf{g}}(t)^{\odot 2} \mathbf{1}_L) \odot \tilde{\mathbf{V}}(t)$ , also follow the gradient flow path. That is:

$$\frac{d}{dt} \tilde{g}_i(t) = -\nabla_{\tilde{g}_i} \mathcal{L}(\tilde{\mathbf{g}}(t), \tilde{\mathbf{V}}(t)), \quad (116)$$

$$\frac{d}{dt} \tilde{V}_{il}(t) = -\nabla_{\tilde{V}_{il}} \mathcal{L}(\tilde{\mathbf{g}}(t), \tilde{\mathbf{V}}(t)). \quad (117)$$

*Proof.* Let the system parameters  $(\tilde{\mathbf{g}}(t), \tilde{\mathbf{V}}(t))$  be derived from the loss function  $\mathcal{L}_N(\tilde{\mathbf{g}}(t), \tilde{\mathbf{V}}(t)) := \|\mathbf{Y} - \mathbf{A}(\tilde{\mathbf{g}}^{\odot 2}(t) \mathbf{1}_L \odot \tilde{\mathbf{V}}(t))\|$ .

The objective of this proof is to demonstrate that the  $N$ -component trajectory  $(\tilde{g}(t), \tilde{V}(t))$  (which is constructed by embedding a  $K$ -component system  $(\bar{\mathbf{g}}(t), \bar{\mathbf{V}}(t))$  and padding it with zeros) follows the gradient flow dynamics derived from the  $N$ -component loss function,  $\mathcal{L}_N(\tilde{\mathbf{g}}(t), \tilde{\mathbf{V}}(t))$ .

The proof is divided into two parts, considering the components within the support set ( $i \in \mathcal{S}_K$ ) and those outside of it ( $i \notin \mathcal{S}_K$ ).

For the components within the support set ( $i \in \mathcal{S}_K$ ): Let  $k$  be the index such that  $i$  is the  $k$ -th element in the ordered support set  $\mathcal{S}_K$ . Recall that the gradient flow for  $\bar{g}_k(t)$  is related to the gradient as:

$$\frac{d}{dt} \bar{g}_k(t) = -\nabla_{\bar{g}_k(t)} \mathcal{L}_K(\bar{\mathbf{g}}(t), \bar{\mathbf{V}}(t)). \quad (118)$$

Substituting the definition of  $\mathcal{L}_K(\cdot, \cdot)$ :

$$\frac{d}{dt} \bar{g}_k(t) = -\nabla_{\bar{g}_k(t)} \left( \sum_m \sum_l \left( (Y_{ml} - \sum_{j \in [K]} \bar{A}_{mj} \bar{g}_j^2(t) \bar{V}_{jl}(t) \right)^2 \right). \quad (119)$$

Taking the derivative:

$$\frac{d}{dt} \bar{g}_k(t) = 4\bar{g}_k(t) \sum_m \sum_l \bar{A}_{mk} \left( Y_{ml} - \sum_{j \in [K]} \bar{A}_{mj} \bar{g}_j^2(t) \bar{V}_{jl}(t) \right) \bar{V}_{kl}(t), \quad (120)$$

By the definition of parameters, we can replace the  $K$ -component parameters  $\bar{g}_k(t)$ ,  $\bar{V}_{kl}(t)$  and the columns of  $\bar{\mathbf{A}}$  by their corresponding  $N$ -component parameters  $\tilde{g}_i(t)$ ,  $\tilde{V}_{il}(t)$  and columns of  $\mathbf{A}$ .

$$\frac{d}{dt} \bar{g}_k(t) = 4\tilde{g}_i(t) \sum_m \sum_l A_{mi} \left( Y_{ml} - \sum_{j \in \mathcal{S}_K} A_{mj} \tilde{g}_j^2(t) \tilde{V}_{jl}(t) \right) \tilde{V}_{il}(t). \quad (121)$$

For any  $j \notin \mathcal{S}_K$ , we have  $\tilde{g}_j(t) = 0$ ,  $\tilde{V}_{jl}(t) = 0$ , hence we can also write it as

$$\frac{d}{dt} \bar{g}_k(t) = 4\tilde{g}_i(t) \sum_m \sum_l A_{mi} \left( Y_{ml} - \sum_{j \in [N]} A_{mj} \tilde{g}_j^2(t) \tilde{V}_{jl}(t) \right) \tilde{V}_{il}(t), \quad (122)$$

This expression is the negative partial derivative of the loss function  $(\mathcal{L}_N(\tilde{\mathbf{g}}(t), \tilde{\mathbf{V}}(t))$  with respect to  $\tilde{g}_i(t)$  i.e.,

$$\frac{d}{dt} \bar{g}_k(t) = -\nabla_{\tilde{g}_i(t)} \sum_m \sum_l \left( Y_{ml} - \sum_{j \in [N]} A_{mj} \tilde{g}_j^2(t) \tilde{V}_{jl}(t) \right)^2, \quad (123)$$

$$= -\nabla_{\tilde{g}_i(t)} \mathcal{L}_N(\tilde{\mathbf{g}}(t), \tilde{\mathbf{V}}(t)). \quad (124)$$

By the definition (114), we have:

$$\frac{d}{dt} \tilde{g}_i(t) = \frac{d}{dt} \bar{g}_k(t). \quad (125)$$

Thus combining the results from (124) and (125), we have:

$$\frac{d}{dt} \tilde{g}_i(t) = -\nabla_{\tilde{g}_i} \mathcal{L}_N(\tilde{\mathbf{g}}(t), \tilde{\mathbf{V}}(t)). \quad (126)$$

Following the same line of reasoning, we begin with the gradient flow for  $\bar{V}_{kl}(t)$

$$\frac{d}{dt} \bar{V}_{kl}(t) = -\nabla_{\bar{V}_{kl}(t)} \mathcal{L}_K(\bar{\mathbf{g}}(t), \bar{\mathbf{V}}(t)), \quad (127)$$

$$= -\nabla_{\bar{V}_{kl}} \left( \sum_m \sum_l \left( Y_{ml} - \sum_{j \in [K]} \bar{A}_{mj} \bar{g}_j^2(t) \bar{V}_{jl}(t) \right)^2 \right) \quad (128)$$

$$= 2\bar{g}_k^2(t) \sum_m \bar{A}_{mk} \left( Y_{ml} - \sum_{j \in [K]} \bar{A}_{mj} \bar{g}_j^2(t) \bar{V}_{jl}(t) \right) \quad (129)$$

$$= 2\tilde{g}_i^2(t) \sum_m A_{mi} \left( Y_{ml} - \sum_{j \in \mathcal{S}_K} A_{mj} \tilde{g}_j^2(t) \tilde{V}_{jl}(t) \right). \quad (130)$$

The last line is obtained by replacing the  $K$ -component parameters by their  $N$ -component counterparts.

For any  $j \notin \mathcal{S}_K$ , we have  $\tilde{g}_j(t) = 0, \tilde{V}_{jl}(t) = 0$ , hence we can also write the above as

$$\frac{d}{dt} \bar{V}_{kl}(t) = 2\tilde{g}_i^2(t) \sum_m A_{mi} \left( Y_{ml} - \sum_{j \in [N]} A_{mj} \tilde{g}_j^2(t) \tilde{V}_{jl}(t) \right), \quad (131)$$

This expression is the negative partial derivative of the loss function  $(\mathcal{L}_N(\tilde{\mathbf{g}}(t), \tilde{\mathbf{V}}(t)))$  with respect to  $\tilde{V}_{il}(t)$  i.e.,

$$\frac{d}{dt} \bar{V}_{kl}(t) = -\nabla_{\tilde{V}_{il}(t)} \sum_m \sum_l \left( Y_{ml} - \sum_{j \in [N]} A_{mj} \tilde{g}_j^2(t) \tilde{V}_{jl}(t) \right)^2, \quad (132)$$

$$= -\nabla_{\tilde{V}_{il}} \mathcal{L}_N(\tilde{\mathbf{g}}(t), \tilde{\mathbf{V}}(t)). \quad (133)$$

By the definition (114), we have

$$\frac{d}{dt} \tilde{V}_{il}(t) = \frac{d}{dt} \bar{V}_{kl}(t). \quad (134)$$

Combining the results from (133) and (134) we have:

$$\frac{d}{dt} \tilde{V}_{kl}(t) = -\nabla_{\tilde{V}_{il}(t)} \mathcal{L}_N(\tilde{\mathbf{g}}, \tilde{\mathbf{V}}). \quad (135)$$

For the components outside the support set ( $i \notin \mathcal{S}_K$ ):

By definitions (114) and (115),  $\tilde{g}_i(t) = 0$  and  $\tilde{V}_{il}(t) = 0$  for all  $t \geq 0$ . Also, note that  $\nabla_{\tilde{V}_{il}(t)} \mathcal{L}_N(\tilde{\mathbf{g}}(t), \tilde{\mathbf{V}}(t)) \propto \tilde{g}_i^2(t)$  and  $\nabla_{\tilde{g}_i(t)} \mathcal{L}_N(\tilde{\mathbf{g}}(t), \tilde{\mathbf{V}}(t)) \propto \tilde{g}_i(t)$ . Combining we arrive at:

$$\frac{d}{dt} \tilde{g}_i(t) = 0 = -\nabla_{\tilde{g}_i(t)} \mathcal{L}_N(\tilde{\mathbf{g}}(t), \tilde{\mathbf{V}}(t)), \quad (136)$$

and

$$\frac{d}{dt} \tilde{V}_{il}(t) = 0 = -\nabla_{\tilde{V}_{il}(t)} \mathcal{L}_N(\tilde{\mathbf{g}}(t), \tilde{\mathbf{V}}(t)). \quad (137)$$

Thus, from equations (126), (135), (136), and (137) we have that  $\tilde{\mathbf{g}}(t)$  and  $\tilde{\mathbf{V}}(t)$  both follow gradient flow path on  $N$  component.  $\square$

**Lemma C.2** (Lemma 5.5 restated). *Let the estimated trajectory,  $\mathbf{X}(t)$  be parametrized by  $(\mathbf{g}(t), \mathbf{V}(t))$  and a reference trajectory  $\tilde{\mathbf{X}}(t)$ , be parameterized by  $(\tilde{\mathbf{g}}(t), \tilde{\mathbf{V}}(t))$  both of which evolve under the continuous gradient flow, as described in Lemma 5.1. Let  $T > 0$  and  $D > 0$  scalars. Specifically, assume that for all  $t \in [0, T]$  and all  $n \in [N]$ , the condition  $\max \left\{ |g_n(t)|, \|V_{n:}(t)\|_2, |\tilde{g}_n(t)|, \|\tilde{V}_{n:}(t)\|_2 \right\} \leq D$  holds.*

At any time  $t \in [0, T]$ , the following inequality holds:

$$\left\| \mathbf{X}(t) - \tilde{\mathbf{X}}(t) \right\|_F^2 \leq 8D^4 \left\| (\mathbf{g}(t), \mathbf{V}(t)) - (\tilde{\mathbf{g}}(t), \tilde{\mathbf{V}}(t)) \right\|^2, \quad (138)$$

where,  $\left\| (\mathbf{g}(t), \mathbf{V}(t)) - (\tilde{\mathbf{g}}(t), \tilde{\mathbf{V}}(t)) \right\|^2 = \sum_{n \in [N]} \sum_{l \in [L]} \left( (V_{nl}(t) - \tilde{V}_{nl}(t))^2 + (g_n(t) - \tilde{g}_n(t))^2 \right)$ .

*Proof.*

$$\left\| \mathbf{X}(t) - \tilde{\mathbf{X}}(t) \right\|_F^2 = \sum_{n \in [N]} \left\| g_n^2(t) \mathbf{V}_{n:}(t) - \tilde{g}_n^2(t) \tilde{\mathbf{V}}_{n:}(t) \right\|_2^2 \quad (139)$$

$$= \sum_{n \in [N]} \left\| g_n^2(t) \mathbf{V}_{n:}(t) + g_n^2(t) \tilde{\mathbf{V}}_{n:}(t) - g_n^2(t) \tilde{\mathbf{V}}_{n:}(t) - \tilde{g}_n^2(t) \tilde{\mathbf{V}}_{n:}(t) \right\|_2^2 \quad (140)$$

$$= \sum_{n \in [N]} \left\| g_n^2(t) \left( \mathbf{V}_{n:}(t) - \tilde{\mathbf{V}}_{n:}(t) \right) + \tilde{\mathbf{V}}_{n:}(t) (g_n^2(t) - \tilde{g}_n^2(t)) \right\|_2^2 \quad (141)$$

$$\leq \sum_{n \in [N]} \left( g_n^2(t) \left\| \mathbf{V}_{n:}(t) - \tilde{\mathbf{V}}_{n:}(t) \right\|_2 + \left\| \tilde{\mathbf{V}}_{n:}(t) \right\|_2 |(g_n^2(t) - \tilde{g}_n^2(t))| \right)^2, \quad (142)$$

using  $(a + b)^2 \leq 2a^2 + 2b^2$ ,

$$\left\| \mathbf{X}(t) - \tilde{\mathbf{X}}(t) \right\|_F^2 \leq 2 \sum_{n \in [N]} \left( (g_n^2(t))^2 \left\| \mathbf{V}_{n:}(t) - \tilde{\mathbf{V}}_{n:}(t) \right\|_2^2 + \left\| \tilde{\mathbf{V}}_{n:}(t) \right\|_2^2 (g_n^2(t) - \tilde{g}_n^2(t))^2 \right) \quad (143)$$

$$\leq 2 \sum_{n \in [N]} \left( g_n^4(t) \sum_{l \in [L]} \left( V_{nl}(t) - \tilde{V}_{nl}(t) \right)^2 + \sum_{l \in [L]} \tilde{V}_{nl}(t)^2 ((g_n(t) - \tilde{g}_n(t)) (g_n(t) + \tilde{g}_n(t)))^2 \right) \quad (144)$$

Using the inequalities  $\{|g_n(t)|, \|V_{n:}(t)\|_2\} \leq D$  and  $\{\|\tilde{g}_n(t)\|, \|\tilde{V}_{n:}(t)\|_2\} \leq D$ , we can write the above equation as:

$$\left\| \mathbf{X}(t) - \tilde{\mathbf{X}}(t) \right\|_F^2 \leq 2 \sum_{n \in [N]} \sum_{l \in [L]} \left( D^4 \left( V_{nl}(t) - \tilde{V}_{nl}(t) \right)^2 + 4D^4 (g_n(t) - \tilde{g}_n(t))^2 \right) \quad (145)$$

$$\leq 8D^4 \sum_{n \in [N]} \sum_{l \in [L]} \left( \left( V_{nl}(t) - \tilde{V}_{nl}(t) \right)^2 + (g_n(t) - \tilde{g}_n(t))^2 \right) \quad (146)$$

Using the squared parameter distance defined in equation (79):

$$\leq 8D^4 \left\| (\mathbf{g}(t), \mathbf{V}(t)) - (\tilde{\mathbf{g}}(t), \tilde{\mathbf{V}}(t)) \right\|^2. \quad (147)$$

□

### C.1. Proof of Theorem 5.6

To prove the theorem, our strategy is to first construct an idealized, reference low-rank trajectory, denoted as  $\tilde{\mathbf{X}}(t)$ , which will serve as a theoretical benchmark. This trajectory is designed to be perfectly rank- $K$  by initializing it such that only the rows within a specific support set,  $\mathcal{S}_K$ , are non-zero. The initial magnitude of these non-zero rows is controlled by a small positive scalar,  $\rho$ .

The core of our proof will now be to show that the estimated trajectory found by the algorithm, namely,  $\mathbf{X}(t)$ , remains close to this reference trajectory, namely,  $\tilde{\mathbf{X}}(t)$ , provided the initialization is sufficiently small. It is crucial to note that estimated trajectory,  $\mathbf{X}(t)$ , does not assume any knowledge of the support set  $\mathcal{S}_K$  or sparsity level  $K$ .

A standard approach to bounding the divergence between the two trajectories is to employ Grönwall's inequality (Razin et al., 2021). However, this technique yields an error bound that grows exponentially with time. This forces the initializations to be set far below the machine precision, rendering the theoretical guarantees practically unrealizable.

To address this, we construct a Lyapunov function,  $\mathcal{E}(t)$ . This approach allows us to track the divergence more tightly, leading to a bound that linearly  $t$  rather than exponentially. Consequently, we derive convergence guarantees that hold for initializations that are numerically implementable.

We begin the proof using the idealized rank- $K$  trajectory,  $\tilde{\mathbf{X}}(t)$  as in (113). This initialization along with Corollary 5.4 and Lemma B.7 ensures that the rows outside the support  $\mathcal{S}_K$  are initialized at zero and remain zero under the gradient flow dynamics. Thus,  $\tilde{\mathbf{X}}(t)$  is guaranteed to be an at-most rank- $K$  matrix for all  $t \geq 0$ .

To quantify the proximity between the estimated parameters  $(\mathbf{g}(t), \mathbf{V}(t))$  and reference parameters  $(\tilde{\mathbf{g}}(t), \tilde{\mathbf{V}}(t))$ , we use the squared distance,  $\|(\mathbf{g}(t), \mathbf{V}(t)) - (\tilde{\mathbf{g}}(t), \tilde{\mathbf{V}}(t))\|^2$ .

We formally define the Lyapunov function  $\mathcal{E}(t)$  as:

$$\mathcal{E}(t) = \|(\mathbf{g}(t), \mathbf{V}(t)) - (\tilde{\mathbf{g}}(t), \tilde{\mathbf{V}}(t))\|^2 = \sum_{i \in [N]} \sum_{l \in [L]} (|g_i(t) - \tilde{g}_i(t)|^2 + |V_{il}(t) - \tilde{V}_{il}(t)|^2) \quad (148)$$

We decompose this into summation of independent row-wise components,  $\mathcal{E}_i(t)$ , corresponding to each row index  $i \in [N]$ :

$$\mathcal{E}(t) = \sum_{i \in [N]} \mathcal{E}_i(t) \quad (149)$$

$$\text{where } \mathcal{E}_i(t) = \sum_{l \in [L]} (|g_i(t) - \tilde{g}_i(t)|^2 + |V_{il}(t) - \tilde{V}_{il}(t)|^2), \quad \forall i \in [N] \quad (150)$$

### C.1.1. BOUNDING THE ERROR ON NON-SUPPORT INDICES ( $i \notin \mathcal{S}_K$ )

We begin by analyzing the error growth on the non-support indices/rows ( $i \notin \mathcal{S}_K$ ). For these rows, the reference trajectory is zero (by construction  $\tilde{g}_i(0) = 0, \tilde{V}_{il}(0) = 0$  and its subsequent updates  $\tilde{g}_i(t) = 0, \tilde{V}_{il}(t) = 0$  as a consequence of Lemma C.1). Consequently, the row-wise error term simplifies to the energy of estimated trajectory alone.

$$\mathcal{E}_i(t) = \mathcal{E}_{e_i}(t) = \sum_{l \in [L]} (g_i(t)^2 + V_{il}(t)^2) \quad (151)$$

From perfect row-balancedness property, i.e.,  $\left(\frac{1}{2}g_i^2(t) = \sum_{l \in [L]} V_{il}^2(t)\right)$ , error in terms of  $|g_i(t)|$  is expressed as

$$\mathcal{E}_{e_i}(t) = \left(L + \frac{1}{2}\right) |g_i(t)|^2 \quad (152)$$

At initialization ( $t = 0$ ), the error is given by:

$$\mathcal{E}_{e_i}(0) = \left(L + \frac{1}{2}\right) \alpha_g^2 = 2L \left(L + \frac{1}{2}\right) \alpha_V^2 \quad (153)$$

Next, to bound the growth of error, we differentiate with respect to time on both sides:

$$\frac{d}{dt} \mathcal{E}_{e_i}(t) = \sum_{l \in [L]} \left( \frac{d}{dt} g_i(t)^2 + \frac{d}{dt} V_{il}(t)^2 \right) \quad (154)$$

$$\frac{d}{dt} \mathcal{E}_{e_i}(t) = \left( L \frac{d}{dt} g_i(t)^2 + \frac{d}{dt} \sum_{l \in [L]} V_{il}(t)^2 \right) \quad (155)$$

From equation (41), (i.e.  $\left(\frac{1}{2} \frac{d}{dt} g_i^2(t) = \frac{d}{dt} \|\mathbf{V}_{i:}(t)\|_2^2 = \frac{d}{dt} \sum_{l \in [L]} V_{il}^2\right)$

$$\frac{d}{dt} \mathcal{E}_{e_i}(t) = \left( L + \frac{1}{2} \right) \left( \frac{d}{dt} g_i(t)^2 \right) \quad (156)$$

$$\frac{d}{dt} \mathcal{E}_{e_i}(t) = 2 \left( L + \frac{1}{2} \right) \left( g_i(t) \frac{d}{dt} g_i(t) \right) \quad (157)$$

$$\begin{aligned}
 \text{Substituting the gradient flow dynamics for } g_i(t) \text{ from equation (34) } \left( \frac{d}{dt} g_i(t) = 4g_i(t) \sum_{j \in [L]} \Lambda_{ij}(t) V_{lj}(t) \right): \\
 = \left( L + \frac{1}{2} \right) 8g_i^2(t) \sum_{l \in [L]} \Lambda_{il}(t) V_{il}(t)
 \end{aligned} \tag{158}$$

Applying Cauchy-Schwarz inequality yields the following upper-bound:

$$\leq \left( L + \frac{1}{2} \right) 8g_i^2(t) \|\Lambda_{i:}(t)\|_2 \|\mathbf{V}_{i:}(t)\|_2 \tag{159}$$

To establish an upper bound on the residual term  $\|\Lambda_{i:}(t)\|_2$ , we leverage the monotonic decrease of the loss function (Ji & Telgarsky, 2019).

$$\|\Lambda_{i:}(t)\|_2 = \|\mathbf{A}_{i:}^\top (\mathbf{Y} - \mathbf{AX}(t))\|_2 \stackrel{(a)}{\leq} \|\mathbf{A}_{i:}^\top\|_2 \|\mathbf{Y} - \mathbf{AX}(t)\|_F \stackrel{(b)}{\leq} \|\mathbf{Y} - \mathbf{AX}(0)\|_F \tag{160}$$

$$\leq \|\mathbf{Y}\|_F + \|\mathbf{A}\|_F \|\mathbf{X}(0)\|_F \stackrel{(c)}{\leq} \|\mathbf{Y}\|_F + N\sqrt{L}\alpha_g^2\alpha_V = \|\mathbf{Y}\|_F + 2L^{3/2}N\alpha_V^3 := C_\Lambda \tag{161}$$

Where <sup>(a)</sup> follows from sub-multiplicativity (Belitskii et al., 2013) of the Frobenius norm (which is a direct consequence of the Cauchy-Schwarz inequality applied column-wise), <sup>(b)</sup> from the  $\ell_2$  normalization of columns of  $\mathbf{A}$  and the monotonic decrease of loss and <sup>(c)</sup> from equation (110) Recall that the gradient flow preserves row-wise balancedness,  $\left( \frac{1}{2}g_i(t)^2 = \sum_{j \in [L]} V_{ij}(t)^2 \right)$ .

Substituting the above derived bound for  $\|\Lambda_{i:}(t)\|_2$  and balancedness into equation (159), we obtain

$$\frac{d}{dt} \mathcal{E}_{e_i}(t) \leq 4\sqrt{2} \left( L + \frac{1}{2} \right) C_\Lambda |g_i(t)|^3 \tag{162}$$

From equation (153), we can substitute for  $|g_i(t)| = (L + \frac{1}{2})^{-1/2} \mathcal{E}_{e_i}(t)^{1/2}$ . Then the bound becomes

$$\frac{d}{dt} \mathcal{E}_{e_i}(t) \leq 4\sqrt{2} \left( L + \frac{1}{2} \right)^{-\frac{1}{2}} C_\Lambda \mathcal{E}_{e_i}^{3/2}(t) = C'_\Lambda \mathcal{E}_{e_i}^{3/2}(t) \tag{163}$$

where,  $C'_\Lambda := 4\sqrt{2} \left( L + \frac{1}{2} \right)^{-\frac{1}{2}} C_\Lambda$ . Rearranging the terms to separate the variables  $\mathcal{E}_{e_i}$  and  $t$  in equation (163), we obtain:

$$\mathcal{E}_{e_i}^{-3/2}(t) \frac{d\mathcal{E}_{e_i}(t)}{dt} \leq C'_\Lambda \tag{164}$$

$$\int_0^t \mathcal{E}_{e_i}^{-3/2}(\tau) \frac{d\mathcal{E}_{e_i}(\tau)}{d\tau} d\tau \leq \int_0^t C'_\Lambda d\tau \tag{165}$$

$$\int_{\mathcal{E}_{e_i}(0)}^{\mathcal{E}_{e_i}(t)} u^{-3/2} du \leq C'_\Lambda t \tag{165}$$

$$\left[ -2u^{-1/2} \right]_{\mathcal{E}_{e_i}(0)}^{\mathcal{E}_{e_i}(t)} \leq C'_\Lambda t \tag{165}$$

$$-2\mathcal{E}_{e_i}^{-1/2}(t) + 2\mathcal{E}_{e_i}^{-1/2}(0) \leq C'_\Lambda t \tag{166}$$

Isolating the term involving  $\mathcal{E}_{e_i}(t)$ :

$$\mathcal{E}_{e_i}^{-1/2}(t) \geq \mathcal{E}_{e_i}^{-1/2}(0) - \frac{1}{2} C'_\Lambda t \tag{167}$$

Taking the reciprocal and squaring both sides yields the upper bound:

$$\mathcal{E}_{e_i}(t) \leq \frac{1}{\left( \mathcal{E}_{e_i}^{-1/2}(0) - \frac{1}{2} C'_\Lambda t \right)^2} \tag{168}$$

C.1.2. BOUNDING THE ERROR ON SUPPORT INDICES ( $i \in \mathcal{S}_K$ )

We now extend our analysis to the rows in the support set  $\mathcal{S}_K$ . Unlike the non-support indices where the reference trajectory remains zero, here the reference trajectory  $\tilde{\mathbf{X}}(t)$  evolves non-trivially according to the gradient flow dynamics. To bound the divergence for these indices, we decompose the total error  $\mathcal{E}_i(t)$  into three distinct components: the energy of the estimated trajectory  $\mathcal{E}_{e_i}(t)$ , the energy of the reference trajectory  $\mathcal{E}_{r_i}(t)$ , and a cross-term  $\mathcal{E}_{x_i}(t)$ . For each row,  $i \in \mathcal{S}_k$ :

$$\mathcal{E}_i(t) = \sum_{l \in [L]} \left( (g_i(t) - \tilde{g}_i(t))^2 + (V_{il}(t) - \tilde{V}_{il}(t))^2 \right) \quad (169)$$

Expanding the squared terms and regrouping the components, we obtain:

$$= \sum_{l \in [L]} \left( g_i^2(t) + \tilde{g}_i^2(t) - 2g_i(t)\tilde{g}_i(t) + V_{il}^2(t) + \tilde{V}_{il}^2(t) - 2V_{il}(t)\tilde{V}_{il}(t) \right) \quad (170)$$

$$= \mathcal{E}_{e_i}(t) + \mathcal{E}_{r_i}(t) - 2\mathcal{E}_{x_i}(t) \quad (171)$$

where the reference energy  $\mathcal{E}_{r_i}(t)$  and the cross-term energy  $\mathcal{E}_{x_i}(t)$  are defined as:

$$\mathcal{E}_{r_i}(t) = \sum_{l \in [L]} \left( \tilde{g}_i(t)^2 + \tilde{V}_{il}(t)^2 \right), \quad (172)$$

$$\mathcal{E}_{x_i}(t) = \sum_{l \in [L]} \left( g_i(t)\tilde{g}_i(t) + V_{il}(t)\tilde{V}_{il}(t) \right). \quad (173)$$

First we bound the energy of the reference trajectory,  $\mathcal{E}_{r_i}(t)$ .

Similar to the approach for the estimated trajectory, we utilize the perfect row-balancedness to express the energy in terms of the scaling factor  $\tilde{g}_i(t)$ :

$$\mathcal{E}_{r_i}(t) = \sum_{l \in [L]} \left( \tilde{g}_i(t)^2 + \tilde{V}_{il}(t)^2 \right) \quad (174)$$

$$\mathcal{E}_{r_i}(t) = \left( L + \frac{1}{2} \right) \tilde{g}_i(t)^2 \quad (175)$$

At time  $t = 0$ , the error is

$$\mathcal{E}_{r_i}(0) = (2L + 1) \rho^{2/3} \quad (176)$$

To bound the growth of energy, we differentiate with respect to time. Substituting the gradient flow dynamics (Lemma C.1) and applying the Cauchy-Schwarz inequality yields the following upper bound:

$$\frac{d}{dt} \mathcal{E}_{r_i}(t) = \left( L + \frac{1}{2} \right) \left( \frac{d}{dt} \tilde{g}_i(t)^2 \right) \quad (177)$$

$$\leq \left( L + \frac{1}{2} \right) 8\tilde{g}_i^2(t) \|\tilde{\Lambda}_{i:}(t)\|_2 \|\tilde{\mathbf{V}}_{i:}(t)\|_2 \quad (178)$$

where we have utilized  $\left( \frac{d}{dt} \tilde{g}_i(t) = 4\tilde{g}_i(t) \sum_{j \in [L]} \tilde{\Lambda}_{ij}(t) \tilde{V}_{lj}(t) \right)$ .

Now, we establish an upper bound on the residual term  $\|\tilde{\Lambda}_{i:}(t)\|_2$ . Proceeding similarly to the derivation of  $C_\Lambda$ , we leverage the monotonic decrease of the loss function to bound the residual by its initialization values:

$$\|\tilde{\Lambda}_{i:}(t)\|_2 \leq \|\mathbf{Y}\|_F + \|\mathbf{A}\|_F \|\tilde{\mathbf{X}}(0)\|_F \leq \|\mathbf{Y}\|_F + \sqrt{K}N\rho := \tilde{C}_\Lambda \quad (179)$$

Substituting the above bound and perfect row-balancedness, we arrive at the differential inequality:

$$\frac{d}{dt} \mathcal{E}_{r_i}(t) \leq 4\sqrt{2} \left( L + \frac{1}{2} \right) C_\Lambda |\tilde{g}_i(t)|^3 \quad (180)$$

Using equation (175) we can substitute  $|\tilde{g}_i(t)| = (L + \frac{1}{2})^{-1/2} \mathcal{E}_{r_i}(t)^{1/2}$ .

$$\frac{d}{dt} \mathcal{E}_{r_i}(t) \leq 4\sqrt{2} \left( L + \frac{1}{2} \right)^{-\frac{1}{2}} \tilde{C}_\Lambda \mathcal{E}_{r_i}^{3/2}(t) = \tilde{C}'_\Lambda \mathcal{E}_{r_i}^{3/2}(t) \quad (181)$$

$$\text{where, } \tilde{C}'_\Lambda := 4\sqrt{2} \left( L + \frac{1}{2} \right)^{-\frac{1}{2}} \tilde{C}_\Lambda$$

The above differential inequality is structurally identical to the one for the estimated trajectory solved in the sub-section C.1.1. Integrating it over the interval  $[0, t]$  immediately yields the analogous upper bound:

$$\boxed{\mathcal{E}_{r_i}(t) \leq \frac{1}{\left( \mathcal{E}_{r_i}^{-1/2}(0) - \frac{1}{2} \tilde{C}'_\Lambda t \right)^2}}. \quad (182)$$

### Bounding the Cross-Term ( $\mathcal{E}_{x_i}$ ):

Having established upper bounds for the energy of both the estimated and reference trajectories, we now bound the cross-term  $\mathcal{E}_{x_i}(t)$ , which represents the alignment between the estimated and reference trajectories.

Recall the decomposition of the total error  $\mathcal{E}_i(t)$ , which we restate here for brevity:

$$\mathcal{E}_i(t) = \mathcal{E}_{e_i}(t) + \mathcal{E}_{r_i}(t) - 2\mathcal{E}_{x_i}(t). \quad (171)$$

From this relation, to establish an upper bound on the total error  $\mathcal{E}_i(t)$ , we require a lower bound on the cross-term  $\mathcal{E}_{x_i}(t)$ .

$$\mathcal{E}_{x_i}(t) = \sum_{l \in [L]} \left( g_i(t) \tilde{g}_i(t) + V_{il}(t) \tilde{V}_{il}(t) \right) \quad (183)$$

Recall that at  $t = 0$ , the initializations are  $V_{ij}(0) = \alpha_V$ ,  $g_i(0) = \alpha_g = \sqrt{2L}\alpha_V$ ,  $\tilde{g}_i(0) = \sqrt{2}\rho^{1/3}$  and  $\tilde{V}_{ij}(0) = \frac{\rho^{1/3}}{\sqrt{L}}$ . The initial cross-term energy is

$$\mathcal{E}_{x_i}(0) = \sqrt{L}(2L+1)\alpha_V\rho^{1/3} \quad (184)$$

Differentiating with respect to time and substituting the gradient flow dynamics as before:

$$\frac{d}{dt} \mathcal{E}_{x_i}(t) = \sum_{l \in [L]} g_i(t) \left( \frac{d}{dt} \tilde{g}_i(t) \right) + \left( \frac{d}{dt} g_i(t) \right) \tilde{g}_i(t) + V_{il}(t) \left( \frac{d}{dt} \tilde{V}_{il}(t) \right) + \left( \frac{d}{dt} V_{il}(t) \right) \tilde{V}_{il}(t) \quad (185)$$

$$= \sum_{l \in [L]} \left( 4g_i(t) \tilde{g}_i(t) \sum_{j \in [L]} \tilde{\Lambda}_{ij}(t) \tilde{V}_{ij}(t) + 4g_i(t) \tilde{g}_i(t) \sum_{j \in [L]} \Lambda_{ij}(t) V_{ij}(t) + 2\tilde{g}_i^2(t) V_{il}(t) \tilde{\Lambda}_{il}(t) + 2g_i^2(t) \Lambda_{il}(t) \tilde{V}_{il}(t) \right) \quad (186)$$

Summing over  $l$  allows us to group terms as

$$= 4Lg_i(t) \tilde{g}_i(t) \left( \sum_{j \in [L]} \tilde{\Lambda}_{ij}(t) \tilde{V}_{ij}(t) + \sum_{j \in [L]} \Lambda_{ij}(t) V_{ij}(t) \right) + 2|\tilde{g}_i(t)|^2 \sum_{l \in [L]} V_{il}(t) \tilde{\Lambda}_{il}(t) + 2|g_i(t)|^2 \sum_{l \in [L]} \Lambda_{il}(t) \tilde{V}_{il}(t) \quad (187)$$

Rewriting in terms of inner products:

$$= 4Lg_i(t)\tilde{g}_i(t) \left( \left\langle \tilde{\Lambda}_{i:}(t)\tilde{\mathbf{V}}_{i:}(t) \right\rangle + \left\langle \Lambda_{i:}(t)\mathbf{V}_{i:}(t) \right\rangle \right) + 2\tilde{g}_i^2(t) \left\langle \mathbf{V}_{i:}(t)\tilde{\Lambda}_{i:}(t) \right\rangle + 2g_i^2(t) \left\langle \Lambda_{i:}(t)\tilde{\mathbf{V}}_{i:}(t) \right\rangle \quad (188)$$

Applying the Cauchy-Schwarz-Bunjakowski inequality (Teschl, 2012) ( $|\langle A, B \rangle| \leq \|A\|\|B\| \implies -\|A\|\|B\| \leq \langle A, B \rangle$ ):

$$\geq -4L|g_i(t)|\|\tilde{\Lambda}_{i:}(t)\|\|\tilde{\mathbf{V}}_{i:}(t)\| + \|\Lambda_{i:}(t)\|\|\mathbf{V}_{i:}(t)\| - 2\tilde{g}_i^2(t)\|\mathbf{V}_{i:}(t)\|\|\tilde{\Lambda}_{i:}(t)\| - 2g_i^2(t)\|\Lambda_{i:}(t)\|\|\tilde{\mathbf{V}}_{i:}(t)\| \quad (189)$$

Substituting the bounds  $\|\Lambda_{i:}\| \leq C_\Lambda$  and  $\|\tilde{\Lambda}_{i:}\| \leq \tilde{C}_\Lambda$

$$\geq -4L|g_i(t)|\|\tilde{\Lambda}_{i:}(t)\|\|\tilde{\mathbf{V}}_{i:}(t)\| + C_\Lambda\|\mathbf{V}_{i:}(t)\| - 2\tilde{C}_\Lambda\tilde{g}_i^2(t)\|\mathbf{V}_{i:}(t)\| - 2C_\Lambda(t)g_i^2(t)\|\tilde{\mathbf{V}}_{i:}(t)\| \quad (190)$$

Applying row-balancedness (i.e.,  $\sqrt{2}\|\mathbf{V}_{i:}\| = |g_i(t)|$ )

$$\geq -2\sqrt{2}L|g_i(t)|\|\tilde{\Lambda}_{i:}(t)\|^2\tilde{C}_\Lambda - 2\sqrt{2}L|g_i(t)|^2\|\tilde{\Lambda}_{i:}(t)\|C_\Lambda - \sqrt{2}\tilde{C}_\Lambda\tilde{g}_i^2(t)|g_i(t)| - \sqrt{2}C_\Lambda(t)g_i^2(t)|g_i(t)| \quad (191)$$

Rearranging the terms and factoring out the common scalar components allows us to group the expression as

$$\geq -\sqrt{2}|g_i(t)|\|\tilde{\Lambda}_{i:}(t)\|^2\tilde{C}_\Lambda(2L+1) - \sqrt{2}|g_i(t)|^2\|\tilde{\Lambda}_{i:}(t)\|C_\Lambda(2L+1) \quad (192)$$

Substituting  $(|g_i(t)| = \mathcal{E}_{e_i}(t)^{1/2}\left(L + \frac{1}{2}\right)^{-1/2})$  from equation (152) and  $(|\tilde{g}_i(t)| = \mathcal{E}_{r_i}(t)^{1/2}\left(L + \frac{1}{2}\right)^{-1/2})$  equation (175)

$$\geq -\frac{4}{\sqrt{2L+1}}|\mathcal{E}_{e_i}(t)^{1/2}||\mathcal{E}_{r_i}(t)|\tilde{C}_\Lambda(2L+1) - \frac{4}{\sqrt{2L+1}}|\mathcal{E}_{e_i}(t)||\mathcal{E}_{r_i}(t)^{1/2}|C_\Lambda \quad (193)$$

Furthermore, by substituting the time-dependent upper bounds derived for  $\mathcal{E}_{e_i}(t)$  and  $\mathcal{E}_{r_i}(t)$  (specifically from equations (182) and (168)), we obtain the lower bound in terms of  $t$ :

$$\begin{aligned} &\geq -\frac{4}{\sqrt{2L+1}} \left( \frac{1}{\left| \mathcal{E}_{e_i}^{-1/2}(0) - \frac{1}{2}C'_\Lambda t \right|} \right) \left( \frac{1}{\left( \mathcal{E}_{r_i}^{-1/2}(0) - \frac{1}{2}\tilde{C}'_\Lambda t \right)^2} \right) \tilde{C}_\Lambda \\ &\quad - \frac{4}{\sqrt{2L+1}} \left( \frac{1}{\left( \mathcal{E}_{e_i}^{-1/2}(0) - \frac{1}{2}C'_\Lambda t \right)^2} \right) \left( \frac{1}{\left| \mathcal{E}_{r_i}^{-1/2}(0) - \frac{1}{2}\tilde{C}'_\Lambda t \right|} \right) C_\Lambda \end{aligned} \quad (194)$$

(195)

We observe that the lower bound depends on time-varying denominator terms  $\mathcal{E}_{r_i}^{-1/2}(0) - \frac{1}{2}\tilde{C}'_\Lambda t$  and  $\mathcal{E}_{e_i}^{-1/2}(0) - \frac{1}{2}C'_\Lambda t$ . As system evolves from  $t = 0$ , the bound remain valid as long as denominator avoids singularity. This results in an upper bound on time,  $t$ , for which the analysis holds:

$$\mathcal{E}_{r_i}^{-1/2}(0) - \frac{1}{2}\tilde{C}'_\Lambda t > 0 \implies t < \frac{2}{\tilde{C}'_\Lambda \sqrt{\mathcal{E}_{r_i}(0)}} \quad (196)$$

$$\mathcal{E}_{e_i}^{-1/2}(0) - \frac{1}{2}C'_\Lambda t > 0 \implies t < \frac{2}{C'_\Lambda \sqrt{\mathcal{E}_{e_i}(0)}} \quad (197)$$

Thus the analysis holds for  $t \in [0, T)$  where,  $T = \min \left\{ \frac{2}{C'_\Lambda \sqrt{\mathcal{E}_{e_i}(0)}}, \frac{2}{\tilde{C}'_\Lambda \sqrt{\mathcal{E}_{r_i}(0)}} \right\}$ .

Provided  $t \in [0, T]$ , we can rewrite the lower bound (194) as

$$\begin{aligned} \frac{d}{dt} \mathcal{E}_{x_i}(t) &\geq -\frac{4}{\sqrt{2L+1}} \left( \frac{1}{\mathcal{E}_{e_i}^{-1/2}(0) - \frac{1}{2}C'_\Lambda t} \right) \left( \frac{1}{\left( \mathcal{E}_{r_i}^{-1/2}(0) - \frac{1}{2}\tilde{C}'_\Lambda t \right)^2} \right) \tilde{C}_\Lambda \\ &\quad - \frac{4}{\sqrt{2L+1}} \left( \frac{1}{\left( \mathcal{E}_{e_i}^{-1/2}(0) - \frac{1}{2}C'_\Lambda t \right)^2} \right) \left( \frac{1}{\mathcal{E}_{r_i}^{-1/2}(0) - \frac{1}{2}\tilde{C}'_\Lambda t} \right) C_\Lambda \end{aligned} \quad (198)$$

We now simplify the lower bound derived in (198). A closer inspection of the terms reveals a specific algebraic structure: the expression resembles the derivative of an inverse product, i.e.,  $\frac{d}{dt} \frac{-1}{h(t)f(t)}$ . To exploit this, let us define two auxiliary functions  $h(t) = \mathcal{E}_{e_i}^{-1/2}(0) - \frac{1}{2}C'_\Lambda t$  and  $f(t) = \mathcal{E}_{r_i}^{-1/2}(0) - \frac{1}{2}\tilde{C}'_\Lambda t$ .

Then  $\frac{d}{dt} f(t) = -\frac{1}{2}\tilde{C}'_\Lambda$  and  $\frac{d}{dt} h(t) = -\frac{1}{2}C'_\Lambda$ . Recall that  $\tilde{C}'_\Lambda := 4\sqrt{2}\left(L + \frac{1}{2}\right)^{-\frac{1}{2}}\tilde{C}_\Lambda$  and  $C'_\Lambda := 4\sqrt{2}\left(L + \frac{1}{2}\right)^{-\frac{1}{2}}C_\Lambda$ .

Substituting these equations back into equation (198) and simplifying we get:

$$\frac{d}{dt} \mathcal{E}_{x_i}(t) \geq \frac{h(t) \frac{d}{dt} f(t) + f(t) \frac{d}{dt} h(t)}{h^2(t)f^2(t)} \quad (199)$$

Rewriting the term as the derivative of an inverse product:

$$\frac{d}{dt} \mathcal{E}_{x_i}(t) \geq \frac{d}{dt} \frac{-1}{h(t)f(t)} \quad (200)$$

Integrating both sides with respect to time from 0 to  $t$

$$\int_0^t \frac{d}{d\tau} \mathcal{E}_{x_i}(\tau) d\tau \geq \int_0^t \frac{d}{d\tau} \frac{-1}{h(\tau)f(\tau)} d\tau \quad (201)$$

$$\mathcal{E}_{x_i}(t) - \mathcal{E}_{x_i}(0) \geq \frac{1}{h(0)f(0)} - \frac{1}{h(t)f(t)} \quad (202)$$

Recall that at  $\mathcal{E}_{x_i}(0) = \sqrt{L}(2L+1)\alpha_V\rho^{1/3}$ ,  $h(0) = \mathcal{E}_{e_i}^{-1/2}(0) = \left(\alpha_V\sqrt{L(2L+1)}\right)^{-1}$  and  $f(0) = \mathcal{E}_{r_i}^{-1/2}(0) = (\sqrt{2L+1}\rho^{1/3})^{-1}$ .

$$\mathcal{E}_{x_i}(t) \geq 2\sqrt{L}(2L+1)\alpha_V\rho^{1/3} - \frac{1}{\left(\mathcal{E}_{e_i}^{-1/2}(0) - \frac{1}{2}C'_\Lambda t\right) \left(\mathcal{E}_{r_i}^{-1/2}(0) - \frac{1}{2}\tilde{C}'_\Lambda t\right)} \quad (203)$$

We now combine the bounds (168), (182) and (203) to obtain an upper bound on the error  $\mathcal{E}_i(t)$  for all  $i \in \mathcal{S}_K$ . Recall from equation (169) that the total error decomposes as

$$\mathcal{E}_i(t) = \mathcal{E}_{e_i}(t) + \mathcal{E}_{r_i}(t) - 2\mathcal{E}_{x_i}(t) \quad (169)$$

Substituting the bounds derived from equations (168), (182) and (203):

$$\leq \frac{1}{\left(\mathcal{E}_{e_i}^{-1/2}(0) - \frac{1}{2}C'_\Lambda t\right)^2} + \frac{1}{\left(\mathcal{E}_{r_i}^{-1/2}(0) - \frac{1}{2}\tilde{C}'_\Lambda t\right)^2} + \frac{2}{\left(\mathcal{E}_{e_i}^{-1/2}(0) - \frac{1}{2}C'_\Lambda t\right) \left(\mathcal{E}_{r_i}^{-1/2}(0) - \frac{1}{2}\tilde{C}'_\Lambda t\right)} - 4\sqrt{L}(2L+1)\alpha_V\rho^{1/3} \quad (204)$$

Observe that the first three terms form perfect square:

$$\leq \left( \frac{1}{\mathcal{E}_{e_i}^{-1/2}(0) - \frac{1}{2}C'_\Lambda t} + \frac{1}{\mathcal{E}_{r_i}^{-1/2}(0) - \frac{1}{2}\tilde{C}'_\Lambda t} \right)^2 - 4\sqrt{L}(2L+1)\alpha_V\rho^{1/3} \quad (205)$$

Since the initialization parameters  $\alpha_V$  and  $\rho$  are positive, we can omit this negative term to obtain a simplified upper bound:

$$\mathcal{E}_i(t) = \sum_{l \in [L]} \left( (g_i(t) - \tilde{g}_i(t))^2 + (V_{il}(t) - \tilde{V}_{il}(t))^2 \right) \leq \left( \frac{1}{\mathcal{E}_{e_i}^{-1/2}(0) - \frac{1}{2}C'_\Lambda t} + \frac{1}{\mathcal{E}_{r_i}^{-1/2}(0) - \frac{1}{2}\tilde{C}'_\Lambda t} \right)^2 \quad (206)$$

### C.1.3. BOUNDING THE TOTAL ERROR IN THE PARAMETER-SPACE

Summing over all rows (both support and non-support) allows us to bound the total parameter distance squared,  $\|(\mathbf{g}(t), \mathbf{V}(t)) - (\tilde{\mathbf{g}}(t), \tilde{\mathbf{V}}(t))\|^2$ :

$$\begin{aligned} & \|(\mathbf{g}(t), \mathbf{V}(t)) - (\tilde{\mathbf{g}}(t), \tilde{\mathbf{V}}(t))\|^2 \\ &= \sum_{i \in [N]} \sum_{l \in [L]} (|g_i(t) - \tilde{g}_i(t)|^2 + |V_{il}(t) - \tilde{V}_{il}(t)|^2) \\ &= \sum_{i \in [N] - \mathcal{S}_K} \sum_{l \in [L]} (|g_i(t) - \tilde{g}_i(t)|^2 + |V_{il}(t) - \tilde{V}_{il}(t)|^2) + \sum_{i \in \mathcal{S}_K} \sum_{l \in [L]} (|g_i(t) - \tilde{g}_i(t)|^2 + |V_{il}(t) - \tilde{V}_{il}(t)|^2) \\ &= (N - K)\mathcal{E}_{e_i}(t) + K\mathcal{E}_i(t) \end{aligned} \quad (207)$$

$$\leq \frac{N - K}{\left( \mathcal{E}_{e_i}^{-1/2}(0) - \frac{1}{2}C'_\Lambda t \right)^2} + K \left( \frac{1}{\mathcal{E}_{e_i}^{-1/2}(0) - \frac{1}{2}C'_\Lambda t} + \frac{1}{\mathcal{E}_{r_i}^{-1/2}(0) - \frac{1}{2}\tilde{C}'_\Lambda t} \right)^2 \quad (208)$$

Note that  $\frac{1}{\left( \mathcal{E}_{e_i}^{-1/2}(0) - \frac{1}{2}C'_\Lambda t \right)^2} < \left( \frac{1}{\mathcal{E}_{e_i}^{-1/2}(0) - \frac{1}{2}C'_\Lambda t} + \frac{1}{\mathcal{E}_{r_i}^{-1/2}(0) - \frac{1}{2}\tilde{C}'_\Lambda t} \right)^2$  since all terms are strictly positive. Using this inequality, we can upper bound the error contribution from the non-support rows ( $N - K$  terms) by the strictly larger squared sum expression used for the support rows. Furthermore, since  $N - K < N$ , we can combine the coefficients to simplify the total bound:

$$\leq N \left( \frac{1}{\mathcal{E}_{e_i}^{-1/2}(0) - \frac{1}{2}C'_\Lambda t} + \frac{1}{\mathcal{E}_{r_i}^{-1/2}(0) - \frac{1}{2}\tilde{C}'_\Lambda t} \right)^2 \quad (209)$$

### C.2. From Parameter Error to Signal Reconstruction Error

Finally, to guarantee the recovery of the signal matrix  $\mathbf{X}$ , we translate the error in parameter space into the Frobenius norm of the difference of the estimated trajectory and reference trajectory  $\left( \|\mathbf{X}(t) - \tilde{\mathbf{X}}(t)\|_F^2 \right)$ . Utilizing the result from Lemma C.2, which relates parameter distance to matrix distance for bounded trajectories, we obtain:

$$\|\mathbf{X}(t) - \tilde{\mathbf{X}}(t)\|_F^2 \leq 8D^4 \|(\mathbf{g}(t), \mathbf{V}(t)) - (\tilde{\mathbf{g}}(t), \tilde{\mathbf{V}}(t))\|^2 \quad (210)$$

$$\leq 8D^4 N \left( \frac{1}{\mathcal{E}_{e_i}^{-1/2}(0) - \frac{1}{2}C'_\Lambda t} + \frac{1}{\mathcal{E}_{r_i}^{-1/2}(0) - \frac{1}{2}\tilde{C}'_\Lambda t} \right)^2 \quad (211)$$

$$\|\mathbf{X}(t) - \tilde{\mathbf{X}}(t)\|_F \leq 2\sqrt{2N}D^2 \left( \frac{1}{\mathcal{E}_{e_i}^{-1/2}(0) - \frac{1}{2}C'_\Lambda t} + \frac{1}{\mathcal{E}_{r_i}^{-1/2}(0) - \frac{1}{2}\tilde{C}'_\Lambda t} \right) \quad (212)$$

Note that the right hand side of the equation (212) is monotonically increasing with time  $t$ . To ensure that the error  $\|\mathbf{X}(t) - \tilde{\mathbf{X}}(t)\|_F$  remains bounded by  $\epsilon_{\text{app}}$  until  $t = T$ , we restrict the analysis to a time interval  $t \in [0, T)$  where the bound  $\|\mathbf{X}(t) - \tilde{\mathbf{X}}(t)\|_F \leq \epsilon_{\text{app}}$  holds.

$$2\sqrt{2N}D^2 \left( \frac{1}{\mathcal{E}_{e_i}^{-1/2}(0) - \frac{1}{2}C'_\Lambda T} + \frac{1}{\mathcal{E}_{r_i}^{-1/2}(0) - \frac{1}{2}\tilde{C}'_\Lambda T} \right) \leq \epsilon_{\text{app}} \quad (213)$$

Let us define the worst case constants as  $d(0) := \min \{ \mathcal{E}_{e_i}(0)^{-1/2}, \mathcal{E}_{r_i}(0)^{-1/2} \}$  and  $C_{\max} = \max \{ C'_\Lambda, \tilde{C}'_\Lambda \}$ . Then, at any  $t < T$ , where  $T = \min \left\{ \frac{2}{C'_\Lambda \sqrt{\mathcal{E}_{e_i}(0)}}, \frac{2}{\tilde{C}'_\Lambda \sqrt{\mathcal{E}_{r_i}(0)}} \right\}$ , the bound (213) simplifies to

$$\frac{4\sqrt{2N}D^2}{d(0) - \frac{1}{2}C_{\max}T} \leq \epsilon_{\text{app}} \quad (214)$$

Let  $\rho$  be set such that the initial energy of estimated trajectory is at-least that of the reference trajectory:

$$\mathcal{E}_{e_i}(0) \geq \mathcal{E}_{r_i}(0) \quad (215)$$

$$L(2L+1)\alpha_V^2 \geq (2L+1)\rho^{2/3} \quad (216)$$

$$L^{3/2}\alpha_V^3 \geq \rho \quad (217)$$

Under this setting,  $d(0) = \mathcal{E}_{e_i}(0)^{-1/2} = \left( \alpha_V \sqrt{L(2L+1)} \right)^{-1}$ .

Note that

$$C_{\max} = \max \{ C'_\Lambda, \tilde{C}'_\Lambda \} \quad (218)$$

Substituting the constants  $C'_\Lambda = \frac{8}{\sqrt{2L+1}} (\|\mathbf{Y}\|_F + 2L^{3/2}N\alpha_V^3)$ ,  $\tilde{C}'_\Lambda = \frac{8}{\sqrt{2L+1}} (\|\mathbf{Y}\|_F + \sqrt{K}N\rho)$

$$C_{\max} = \frac{8}{\sqrt{2L+1}} \max \left\{ \|\mathbf{Y}\|_F + 2L^{3/2}N\alpha_V^3, \|\mathbf{Y}\|_F + \sqrt{K}N\rho \right\} \quad (219)$$

$$= \frac{8}{\sqrt{2L+1}} \cdot \left( \|\mathbf{Y}\|_F + N \max \left\{ 2L^{3/2}\alpha_V^3, \sqrt{K}\rho \right\} \right) \quad (220)$$

Substituting the bound (217)

$$C_{\max} \leq \frac{8}{\sqrt{2L+1}} \left( \|\mathbf{Y}\|_F + NL^{3/2}\alpha_V^3 \max \left\{ 2, \sqrt{K} \right\} \right) \quad (221)$$

To ensure that the approximation error  $\epsilon_{\text{app}}$  remains small enough i.e.,  $\epsilon_{\text{app}} \in (0, 1)$ , time  $T$  should satisfy equation (214).

Rewriting equation (214), and substituting the constants,

$$\frac{4\sqrt{2N}D^2}{d(0) - \frac{1}{2}C_{\max}T} < \epsilon_{\text{app}} \quad (222)$$

Rearranging the terms:

$$\frac{4\sqrt{2N}D^2}{\epsilon_{\text{app}}} < d(0) - \frac{1}{2}C_{\max}T \quad (223)$$

Grouping the constants on the right hand side and time dependent term on the other:

$$\frac{1}{2}C_{\max}T < d(0) - \frac{4\sqrt{2N}D^2}{\epsilon_{\text{app}}} \quad (224)$$

Solving for  $T$ :

$$T < 2 \frac{d(0) - \frac{4\sqrt{2N}D^2}{\epsilon_{\text{app}}}}{C_{\max}} \quad (225)$$

Simplifying the numerator and denominator:

$$T < 2 \frac{d(0)\epsilon_{\text{app}} - 4\sqrt{2N}D^2}{\epsilon_{\text{app}}C_{\max}} \quad (226)$$

Substituting constants  $d(0) = \left(\alpha_V \sqrt{L(2L+1)}\right)^{-1}$ ,  $C_{\max} = \frac{8}{\sqrt{2L+1}} \left(\|\mathbf{Y}\|_F + NL^{3/2}\alpha_V^3 \max\left\{2, \sqrt{K}\right\}\right)$

$$T < 2 \frac{\frac{\epsilon_{\text{app}}}{\alpha_V \sqrt{L(2L+1)}} - 4\sqrt{2N}D^2}{\frac{8}{\sqrt{2L+1}}\epsilon_{\text{app}} \left(\|\mathbf{Y}\|_F + NL^{3/2}\alpha_V^3 \max\left\{2, \sqrt{K}\right\}\right)} \quad (227)$$

Simplifying, we have

$$T < \frac{\epsilon_{\text{app}} - \alpha_V 4\sqrt{2NL(2L+1)}D^2}{4\epsilon_{\text{app}}\sqrt{L}\alpha_V \left(\|\mathbf{Y}\|_F + NL^{3/2}\alpha_V^3 \max\left\{2, \sqrt{K}\right\}\right)} \quad (228)$$

To ensure that the upper bound on  $T$  is positive, the numerator should be positive. This limits  $\alpha_V$  as follows:

$$0 < \epsilon_{\text{app}} - \alpha_V 4\sqrt{2NL(2L+1)}D^2 \quad (229)$$

$$\alpha_V 4\sqrt{2NL(2L+1)}D^2 < \epsilon_{\text{app}} \quad (230)$$

$$\alpha_V < \frac{\epsilon_{\text{app}}}{4\sqrt{2NL(2L+1)}D^2} \quad (231)$$

This initialization ensures that the error  $\|\mathbf{X}(t) - \tilde{\mathbf{X}}(t)\|_F$  remains below  $\epsilon_{\text{app}}$  for any time  $t \in [0, T]$ .

### C.3. Proof of Corollary 1

**Corollary C.3** (Corollary 5.7 restated). *Assume the conditions of Theorem 5.6, and in addition assume that all reference trajectories  $\tilde{\mathbf{X}}(t)$  converge to a solution  $\mathbf{X}^* \in \mathbb{R}^{N \times L}$ . This convergence is uniform in the sense that the trajectories are confined to a bounded domain, and for any  $\epsilon_{\text{app}} > 0$  there exists a time  $T_c \leq T$  after which they are all within a distance  $\epsilon_{\text{app}}$  from  $\mathbf{X}^*$ . Then for any  $\epsilon_{\text{app}} > 0$ , if the initialization scales  $\alpha_V, \alpha_g$  are sufficiently small, for any time  $t \in [T_c, T]$  it holds that  $\|\mathbf{X}(t) - \mathbf{X}^*\|_F \leq 2\epsilon_{\text{app}}$*

*Proof.* For  $\epsilon_{\text{app}} > 0$ , there exists a time  $T_c > 0$  after which all the reference trajectories are within a distance of  $\epsilon_{\text{app}}$  from the solution  $\tilde{\mathbf{X}}^*$ . i.e.,

$$\|\tilde{\mathbf{X}}(t) - \mathbf{X}^*\| \leq \epsilon_{\text{app}}. \quad (232)$$

where  $t \geq T_c$ . These reference trajectories are also confined within a ball of radius  $D$ . i.e.,  $\|\tilde{\mathbf{X}}(t)\| \leq D$  for all  $t \geq 0$ . From Theorem 5.6, if initialization scales  $\alpha_V, \alpha_g$  are sufficiently small, then

$$\|\mathbf{X}(t) - \tilde{\mathbf{X}}(t)\| \leq \epsilon_{\text{app}} < 1. \quad (233)$$

This bound holds atleast until  $t \geq T$  or  $\|\mathbf{X}(t)\| \geq D + 1$ . In line with the analysis done by Razin et al. (2021), by the way of contradiction, we show that the second condition cannot hold, namely  $\|\mathbf{X}(t)\| \leq D + 1$  cannot be true for any  $t \in [0, T]$ .

Let  $t' \in [0, T]$  be an initial time at which  $\|\mathbf{X}(t')\| \geq D + 1$ . Since  $t' \leq T$ , the guarantee from Theorem 5.6 is still valid, meaning,  $\|\mathbf{X}(t') - \tilde{\mathbf{X}}(t')\| < 1$ , using the triangle inequality we have:

$$\|\tilde{\mathbf{X}}(t')\| \geq \|\mathbf{X}(t')\| - \|\mathbf{X}(t') - \tilde{\mathbf{X}}(t')\| > (D + 1) - 1 \quad (234)$$

$$> D \quad (235)$$

This is a contradiction to the assumption that  $\tilde{\mathbf{X}}(t)$  is confined to a ball of radius  $D$  for  $t = t'$ . Thus, for all  $t \in [0, T]$ , the guarantee  $\|\mathbf{X}(t) - \tilde{\mathbf{X}}(t)\| \leq \epsilon_{\text{app}}$  holds.

For any time  $t \in [T_c, T]$  we can apply the triangle inequality:

$$\|\mathbf{X}(t) - \mathbf{X}^*\| \leq \|\mathbf{X}(t) - \tilde{\mathbf{X}}(t)\| + \|\tilde{\mathbf{X}}(t) - \mathbf{X}^*\| \leq 2\epsilon_{\text{app}} \quad (236)$$

This completes the proof.  $\square$

## D. Result on MNIST

To demonstrate the efficacy of the proposed algorithm on real-world data, we conduct a recovery experiment on a set of images from the MNIST dataset. The experiment uses the first 100 images from the MNIST dataset, each reshaped into a vector of 784 pixels. The images are normalized to have pixel values between 0 and 1. A random Gaussian sensing matrix  $\mathbf{A}$  of size  $700 \times 784$  with  $\ell_2$ -normalized columns is used to generate the measurements. The measurement matrix  $\mathbf{Y}$  is then computed as  $\mathbf{Y} = \mathbf{A}\mathbf{X}$ , where  $\mathbf{X}$  represents the matrix of vectorized MNIST images. The proposed IR-MMV algorithm is used to recover the images from the measurements  $\mathbf{Y}$  and the sensing matrix  $\mathbf{A}$ . For comparison, we also show the results from the M-OMP, M-SP, M-FOCUSS, AMP-MMV, and M-BSBL algorithms. For M-OMP, M-SP, and AMP-MMV which require prior knowledge of the row sparsity level, it is set to  $K = 300$ . The simulations were performed on the GPU of a desktop computer equipped with an Intel Core i5-7600K processor, 16GB of DDR4 RAM and GeForce GTX 1070 with 8GB RAM. The MNIST dataset was obtained under the Creative Commons Attribution-Share Alike 3.0 license.

As shown in Figure 3, the proposed method successfully recovers the digit images, achieving a visual quality comparable to that of the other approaches without requiring any prior information about the signal sparsity.

## E. Code and Reproducibility

The source code, and instructions needed to reproduce all experimental results are provided in the supplementary material as a ZIP file. All experiments were conducted in a Python 3 environment with dependencies listed in ‘requirements.txt’. To reproduce all results, please follow the detailed instructions in the README.md file included in the ZIP file.

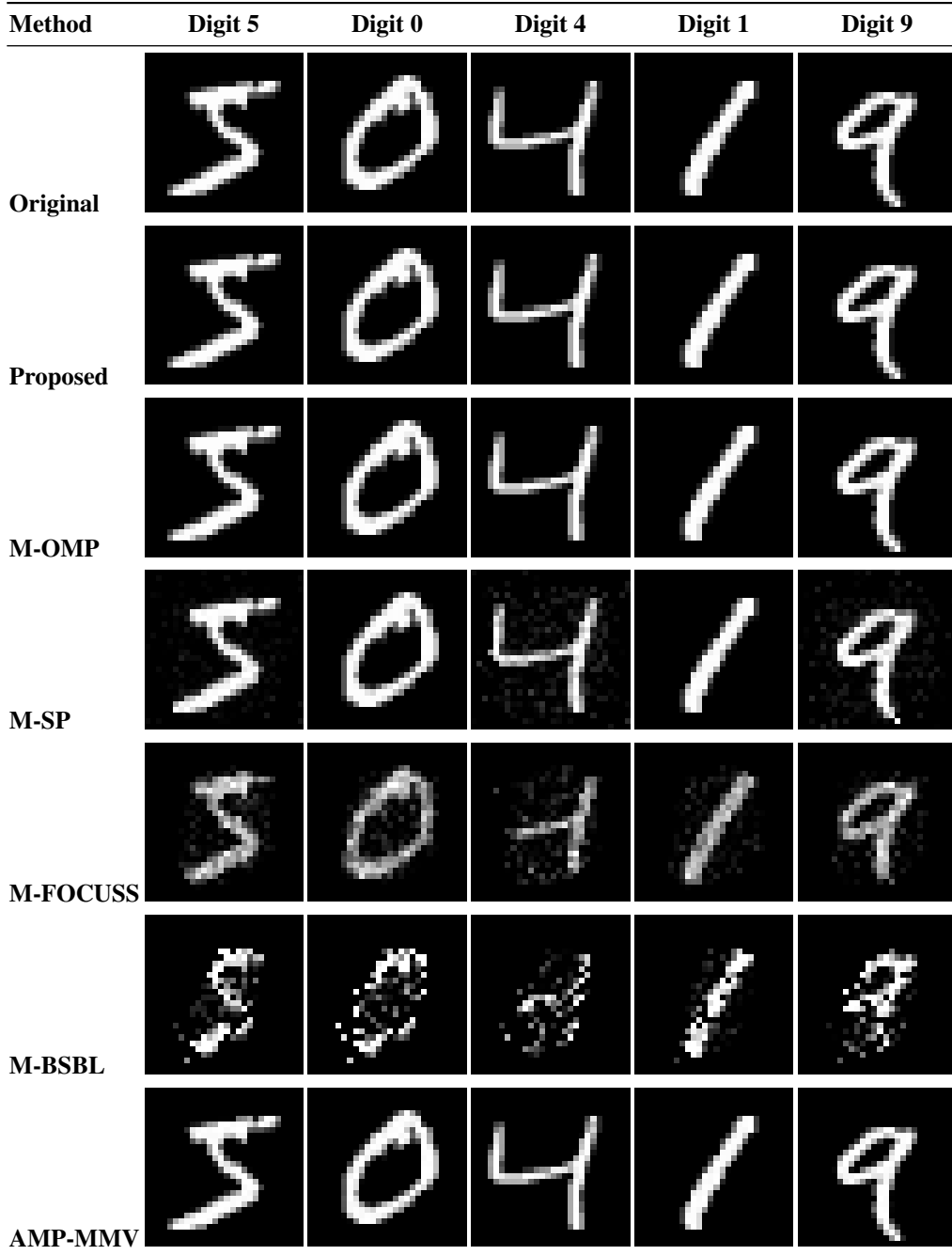


Figure 3. Comparison of MNIST digit reconstruction using different methods. The first row shows the original images.